Progress in Oceanography
November 2019, Volume 178 Pages 102172 (24p.)
https://doi.org/10.1016/j.pocean.2019.102172
https://archimer.ifremer.fr/doc/00511/62293/

Evaluating the ecological status of cold-water coral habitats using non-invasive methods: An example from Cassidaigne canyon, northwestern Mediterranean Sea

Fabri Marie-Claire [1,*], Vinha Beatriz [1], Allais Anne-Gaelle [1], Bouhier Marie-Edith [1], Dugornay Olivier [2], Gaillot Arnaud [2], Arnaubec Aurelien [1]

[1] Ifremer, Centre de Méditerranée, 83500 La Seyne sur Mer, France
[2] Ifremer, Centre de Bretagne, 29280 Plouzané, France

* Corresponding author : Marie-Claire Fabri, email address : Marie.Claire.Fabri@ifremer.fr

Abstract :

Cold-water coral ecosystems have been identified as vulnerable, but quantitative data on their conservation status is very limited. The Marine Strategy Framework Directive (MSFD) is the tool implemented by the European Union's Integrated Maritime Policy to achieve Good Environmental Status (GES) of marine waters by 2020. In this context, the aim of this study was to evaluate the Ecological Status of benthic habitats in Cassidaigne canyon, focusing in particular on cold-water coral habitats dominated by *Madrepora oculata*.

Data were collected during the Videocor1 cruise (2017). Videos and photos collected during eight dives of the H-ROV Ariane were used to reconstruct, in 3-dimensions, the areas where cnidarians have settled in the canyon. A total of 33 3D models were built, which allowed measuring the spatial and vertical distribution, surface, density and size structure of cnidarian populations at four different sites. When 3D reconstructions were not possible, GIS tools were used. The seven cnidarian species considered were the scleractinian *M. oculata*; three antipatharians: *Leiopathes glaberrima*, *Antipathella subpinnata, Antipathes dichotoma*; and three aclyonaceans: the precious red coral *Corallium rubrum* and the gorgonians *Callogorgia verticllata* and *Viminella flagellum*.

Using photogrammetry, we were able to reveal the size structure of the dense population of *M. oculata* in the canyon, as well as to obtain knowledge on a complex site (Cassis-200) composed of 15 knolls, and to quantify the surface occupied by *M. oculata* at a separate site (Cassis-500) influenced by industrial discharges. At the southern flank of the canyon we found a highly diverse site (SW Flank) dominated by antipatharians and gorgonians composing large forests, and finally a reservoir of *M. oculata* was identified under overhangs at a site called the Wall. The diversity of accompanying species is also reported and marine litter quantified. Images collected before 2017 were compared to the 3D models to precisely locate them on the sites, and assess temporal changes in *M. oculata* colony sizes at Cassis-200 site. We also report on the ground-truthing of predicted habitat maps produced previously, and confirm their good representation of the distribution of cold-water coral habitats. Finally, we quantified the criteria defined by the MSFD, aimed at evaluating the GES of benthic habitats for *M. oculata* ecosystems, at the scale of the

Cassidaigne canyon. Measurements showed that the extent of loss of the observed *M. oculata* habitat reached 56% according to the MFSD definition.

Highlights

► Cold-water corals distribution, density and size structure are reported. ► Size measurements were performed using 3D-models. ► A diverse site dominated by antipatharians and gorgonians forests was found. ► The extent of loss of the observed *M. oculata* habitat reached 56%. ► Ground-truthing of predicted habitat maps produced previously is reported.

Keywords : Biodiversity, Photogrammetry, Habitat mapping, Bauxite residues, Vulnerable marine ecosystems

1. Introduction

Cold-water corals encompass many species of the subclass Hexacorallia, including the order of stony corals (Scleractinia) among which are framework-building species, and the order of black corals (Antipatharia) forming arborescent colonies. Some species of the subclass Octocorallia, including gorgonians and alcyonaceans, are also arborescent corals. The two main species known to form complex three-dimensional structures in the Mediterranean Sea are *Lophelia pertusa* and *Madrepora oculata*. These framework-building species can occur in very high densities, increasing habitat heterogeneity thus providing niches for several species at different scales among their polyps, branches, colonies, patches and mounds, and enhancing species density and/or diversity at a local or regional scale (Henry and Roberts, 2017). Framework-building and arborescent corals are very important habitat-structuring species that provide many ecosystem services, by increasing the local biodiversity in the deep Mediterranean Sea (D'Onghia et al., 2010).

Various human activities are known to have a negative effect on cold-water coral communities. Bottom trawling is the most destructive (Benn et al., 2010), and has been banned below 1000 m in the Mediterranean Sea since 2005 (http://www.fao.org/gfcm/data/maps/fras/en/). Although having much less impact than bottom trawling, bottom longlines and gill nets may cause damage to coral colonies when these fishing gears get entangled with corals which are then broken during retrieval of the gear or if gears are lost, trapped in the colonies and moved by water currents. Sediment resuspension and accumulation, seafloor dredging, mineral activities, oil prospection, litter, waste disposal, submarine cables, CO_2-induced global-warming and ocean acidification are other potential threats to the environmental integrity of cold-water coral habitats caused by human activities (Freiwald et al., 2004; Guinotte et al., 2006; McCulloch et al., 2012; Puig et al., 2012; Fabri et al., 2014; Roberts and Cairns, 2014; Lastras et al., 2016). These impacts lead to habitat degradation or destruction and therefore loss or change in biodiversity.

The Marine Strategy Framework Directive (MSFD), adopted in June 2008, commits European Union (EU) Member States to adopt an ecosystem approach to managing the marine environment (European Parliament, 2008). By implementing this directive, the member states aim to achieve good environmental status (GES) of their marine waters by 2020, based on 11 descriptors. This includes deep-sea waters within the European Union Exclusive Economic Zone (EEZ) and embraces, as defined by the MSFD, the water column and the seabed and subsoil under the water column. Monitoring, assessing the environmental status, and managing the deep sea on the basis of knowledge of ecosystem biodiversity, functions and services are crucial actions to ensure its long-term sustainability. Among the 11 descriptors of the MSFD framework, seafloor integrity (D6) is the descriptor used to characterize the status of benthic habitats (European Commission, 2017a, b). Habitat destruction is one of the main threats to environmental integrity (Claudet and Fraschetti,

2010). Assessing the consequences of human impacts is crucial to both predict and prevent structural and functional changes of habitats.

In French Mediterranean waters, structure-forming scleractinians are known from two canyons: Lacaze-Duthiers and Cassidaigne (Fabri et al., 2014). Our study focuses on Cassidaigne canyon, where potential distribution maps of cold-water coral habitat have been produced previously (Fabri et al., 2017; Bargain et al., 2018). These potential suitable areas were inspected in 2017 with a Remotely Operated Vehicle (ROV) to validate the predicted habitat distribution and evaluate the status of populations of different species of benthic megafauna in relation to anthropogenic impacts. For 48 years (1967 to 2015), Cassidaigne canyon was subjected to massive discharges from the aluminum industry, which is known to have had impacts on the local fauna of the canyon (Dauvin, 2010; Fontanier et al., 2012; Fabri et al., 2014; Fontanier et al., 2015; Fabri et al., 2017).

Video and high-resolution images acquired during the 2017 surveys were used to build three-dimensional (3D) models of outcrops on which coral colonies have settled using photogrammetry. The reconstructions of the real-scale 3D models were built from a series of overlapping photos and snapshots of videos (Arnaubec et al., 2015). Photogrammetry provides a permanent record of the 3D coral colonies, gives access to quantitative parameters, replicates measurements and allows monitoring over time. This non-invasive methodology has recently been used for monitoring marine habitats, mostly in shallow waters. For example, it was used to evaluate gorgonian densities and abundances in the Marine Protected Area of Portofino (Palma et al., 2018) and a methodology dedicated to the management and conservation of red coral populations has been formulated (Royer et al., 2018). Regarding deep waters, one study was performed in the Whittard canyon (Atlantic ocean), where photogrammetry was used to highlight the complexity of coral habitats living on vertical walls (Robert et al., 2017). In our study we used photogrammetry to evaluate the ecological status of cold-water coral habitats in Cassidaigne canyon. Our objectives were to:

(1) draw the spatial and vertical distribution of colonial cnidarians (the scleractinian *M. oculata*; the antipatharians: *Leiopathes glaberrima*, *Anthipathella subpinnata* and *Antipathes dichotoma*; the red coral *Corallium rubrum*, and the gorgonians *Callogorgia verticillata* and *Viminella flagellum*);

(2) measure the surface covered by, and the density of, populations of *M. oculata*, *C. rubrum* and gorgonians using photogrammetry and video analyses;

(3) measure the size structure of *M. oculata* and *C. verticillata* populations at different locations in the canyon;

(4) evaluate the diversity of megafauna species at the different locations in the canyon;

(5) quantify the seafloor integrity in areas dominated by *M. oculata* populations at the scale of the Cassidaigne canyon, using the two criteria defined by the MSFD to evaluate the status of benthic habitats;

(6) assess temporal changes in ecological status at a location in Cassidaigne canyon that had been previously surveyed in 2010 and 2013;

(7) validate the habitat suitability model previously built for cold-water corals at the scale of the Cassidaigne canyon.

2. Materials and methods

2.1 Study area

The head of the Cassidaigne canyon (Fig. 1) is located at a depth of 190 m and 8 km away from the coast, in the Eastern part of the Gulf of Lion (NW Mediterranean Sea). In this region, the general water circulation (the Northern Current, from 0 to 200 m depth) follows a westward direction along the continental slope. In the presence of the prevailing Mistral wind (from north or north-west), intense upwelling is generated in the canyon area (Millot, 1990; Alberola and Millot, 2003).

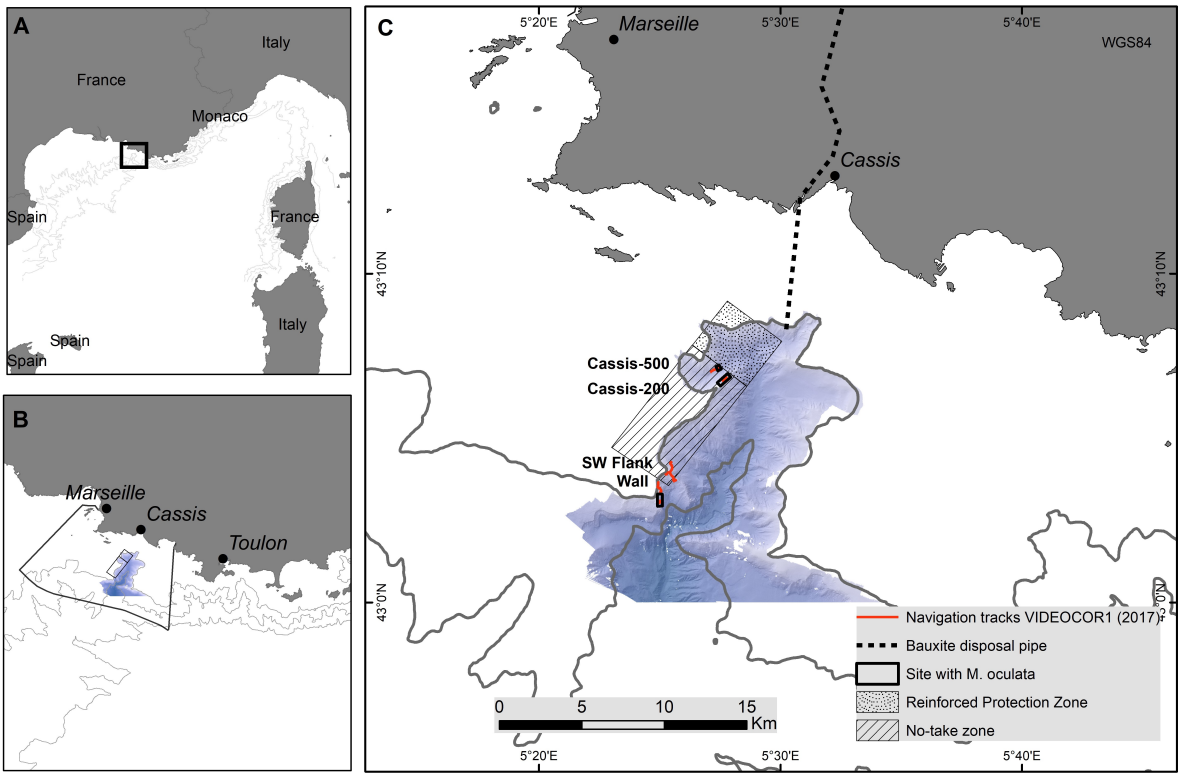

Figure 1: Location map of the study area. A: The global location is the eastern part of the Gulf of Lion; B: the Marine Protected Area (MPA) of the "Parc National des Calanques"; C: The Cassidaigne canyon, the bauxite disposal pipe, the reinforced protection zone and the no-take zone, and the four locations surveyed by the ROV Ariane during the VIDEOCOR1 cruise (2017).

In Cassidaigne canyon, *M. oculata* colonies were previously reported only on exposed bedrock and on vertical walls of the western flank (Fabri et al., 2014; Fabri et al., 2017). Four locations were explored during the Videocor1 cruise (2017): Cassis-200, Cassis-500, SW Flank and the Wall at depths from 200 to 515 meters (Fabri et al., 2017).

Since 1967, the canyon has been impacted by the direct disposal of bauxite residues (red mud) from two different aluminum factories. After 1988 the discharge of bauxite residues was reduced as one

factory stopped production. This disposal is known to have impacts on the local fauna of the canyon (Dauvin, 2010; Fontanier et al., 2012; Fabri et al., 2014; Fontanier et al., 2015; Fabri et al., 2017). Nevertheless, in an attempt to apply the protocols of the Barcelona Convention (1976), the French government decided to stop the disposal of red mud in January 2016, by granting a six-year license for the disposal of a fluid with no suspended matter and only chemicals, instead.

Additionally, to reduce impacts from fisheries, the Cassidaigne canyon is now included in the Marine Protected Area (MPA) of the "Parc National des Calanques" (www.calanques-parcnational.fr – Decree 2012-507). Thus, two zones were created on the western flank of the canyon: a (1) 'reinforced protection zone', i.e. a no-take zone with the exception of local artisanal fisheries, and a (2) 'no-take zone', where no fishing activity is allowed (Fabri et al., 2014).

2.2 Data acquisition

Scientific data were collected during the Videocor1 cruise in 2017. This cruise, on board the scientific R/V L'Europe, was the first to deploy the new Hybrid-ROV Ariane (©Ifremer) (Raugel et al., 2019). Data were obtained from a total of 8 dives (supp. mat. A), with the acquisition of 24 hours of video (10h on Cassis-200, 4h on Cassis-500, 1h30 on the Wall, and 8h30 on SW Flank) and more than 8,000 photos of different rugged sites along the canyon. No *in situ* measurements were performed since a laser measurement system was not available during the cruise. The four locations explored during Videocor1 were chosen based on the results of the habitat suitability models previously built for the canyon (Fabri et al., 2017; Bargain et al., 2018).

Ariane was equipped with an HD photo camera (Nikon D5200) and two video cameras, an HD pan and tilt mounted camera with zoom capacity (Camera Principale) and an HD tilt mounted camera (Camera Science). The navigation data were derived from the acoustic USBL GPS positioning system.

In this study, the 2-meter resolution bathymetry used was that collected locally at the same four sites during the Bathycor 2 cruise (2016) by the Autonomous Underwater Vehicle (AUV) Idef'X (©Ifremer). (DOI: 10.17600/16011300).

2.3 Video and image processing

The videos recorded by Ariane were analyzed either with Matisse and 3D Metrics processing tools (©Ifremer) or Adelie Video (©Ifremer) depending on the type of site (flat or with vertical parts) and the ability to build a 3-dimension (3D) reconstruction or not.

2.3.1 Matisse and 3D Metrics processing tools (Photogrammetry)

The 3D models were built using the 'Structure from motion' technique, based on multi-view geometry and image matching. A global view of the scene can be obtained by building a map using multiple images. This technique uses the redundancy of successive images or within a video flux to put all the pieces together and build the global view (Bruno et al., 2011; Arnaubec et al., 2015).

Limited visibility imposes taking images close to the sea-floor, with a small footprint for each image, and requires artificial illumination of the scene as light is greatly attenuated in water. However, artificial light cannot be optimized to light the scene uniformly, therefore deep-sea optical images

must be compensated for non-uniform illumination. Taking other disturbances such as color dependent attenuation and marine snow into account are part of the preprocessing step. These steps are followed by the construction of a sparse 3D cloud that is then densified. The dense point cloud is used to create a surface (mesh), and then the original images are projected onto the mesh to obtain the final textured model. In order to geo-reference these data and make measurements, the absolute position and scale are obtained by merging the navigation system positioning and the camera positions retrieved during the reconstruction process.

In this study, a total of 33 models were built, when possible based on HD photos collected regularly by automatic acquisition during the cruise. When automatic acquisition had not been triggered, video stills were used instead of photos if needed (supp. mat. A). The 3D Metrics processing tool was used to view the models and measure population parameters.

2.3.2 Adelie Video for georeferencing species occurrences

The Ifremer post-processing software: Adelie Video© was used to analyze videos recorded along linear dive transects where photogrammetry was not useful to map distribution because of the flat shape of the seafloor, such as along the SW-Flank site. This processing allowed georeferencing species occurrence observed on videos using the corresponding navigation file, and mapping the distribution in a GIS (ArcMap ©ESRI).

2.4 Data analysis

2.4.1 Species distribution

The species considered for this study are not only the structure-forming scleractinian *M. oculata*, but also other cold-water coral species providing 3D-habitat to other species: antipatharians *Leiopathes glaberrima*, *Antipathella subpinnata* and *Antipathes dichotoma*; alcyonaceans *C. rubrum* (precious red coral), gorgonians *Callogorgia verticillata* and *Viminella flagellum*.

The distribution of the species considered was obtained using either photogrammetry or video analysis. Each colony was then manually plotted using 3D Metrics or Adelie Video, to obtain the depth, latitude and longitude. In the second step, occurrence points were exported and mapped in ArcMap©ESRI for spatial distribution, or processed in Excel©Microsoft for vertical distribution. Species whose recognition/identification was not easy in the 3D models were plotted with the help of video and HD photos to find their exact position in the reconstructions.

2.4.2 Surface and density

A 3D approach was used to calculate the surface and density occupied by species settled on rocky outcrops with complextopography, i.e. *M. oculata* and *C. rubrum*, and a 2-dimension (2D) approach was used for species seen along linear transects on smooth areas, i.e. *C. verticillata* and *V. flagellum*.

In the 3D approach, a maximum number of colonies of *M. oculata* and *C. rubrum* was plotted on the 3D models, giving the total number of colonies (nb) in each reconstruction. Colonies under 2 cm were not plotted. The surface occupied by the colonies plotted was measured using the polygon function of the 3D Metrics processing tool. This allowed calculating the density of species considering the actual surface area of the bottom taking into account its 3D structure (nb colonies.m^{-2}). The points plotted with 3D Metrics could also be exported and mapped in plan view through GIS. Areas occupied by colonies were then contoured by polygons and the area of each polygon was calculated on a horizontal view. The number of colonies belonging to each polygon was known, which allowed estimating the colony density projected onto a horizontal plane (nb colonies.m^{-2}).

Where colonies were settled under the overhangs of the Wall, it was not possible to take photos because the HD photo camera could not be directed upwards. Therefore, this site was reconstructed using video images from the 'Camera Principale' located on the top of the ROV, which could be directed upwards. The resulting 3D models had low resolution, allowing identification of only a quarter of the individual colonies from the models. However, colonies could be counted using snapshots of the video of the different parts of the huge overhangs.

In the 2D approach, species observed and settled along linear transects, i.e. *C. verticillata* and *V. flagellum,* were plotted in a GIS using Adelie-Video, and a linear density was calculated (nb colonies.m^{-1}). Sections of 20 m-long were calculated using the GIS tool, Adelie-Observation©Ifremer. At Cassis-500, *C. verticillata* was also present but in smaller areas, and thus the sections used were 10 m in length.

No estimation of density and surface could be calculated for antipatharian species, given the difficulty of reconstructing them in 3D, and the difficulty of counting, from video, the total number of individuals forming forests and gardens.

2.4.3 Size

Colony heights were measured using 3D Metrics. Size measurements were performed on *M. oculata, C. rubrum*, *C. verticillata and V. flagellum* populations, in attempts to measure as many colonies as possible in each 3D model. No antipatharian size measurements could be performed since colonies always move with the water flow and local currents, therefore they cannot be represented by 3D reconstructions. Nevertheless, a qualitative description of antipatharian colony sizes was made through video and photo analysis.

2.4.4 Diversity of accompanying species

The different species observed were identified to the lowest taxonomic level possible, using high resolution digital photos and the book "Guide de la faune profonde de la mer Méditerranée" (Fourt et al., 2017). Since no specimen was sampled, some species could not be identified (i.e. sponges), but were morphologically distinguished. Abundances are given as presence and absence data based on species observations at each location.

2.4.6 Statistical analysis

Statistical analysis was performed using XLSTAT 2019 for Excel (Addinsoft, 2019). Box-plots of the vertical distribution of the different species were produced. A non-parametric Kruskal-Wallis test was used to compare mean sizes of *M. oculata* colonies at three locations. Non-parametric Mann-Whitney tests were computed to compare mean sizes of *C. verticillata* colonies at two locations, and the same was applied for *V. flagellum*. Gaussian mixture models were run to identify the different size groups at each location for the same species.

A hierarchical clustering of the four locations was performed based on the presence or absence of species, including habitat-forming cnidarians. The Sorensen similarity coefficient was used to build the similarity matrix because this coefficient is based on binary data, and it emphasizes the presence of species (absence may be due to weak sampling effort).

2.5 Degradation and seafloor integrity

Areas where coral rubble was found were contoured and measured with 3D Metrics, allowing their estimation in 3D, after which they were transferred to a GIS for positioning and measurement in 2D.

Marine litter observations were georeferenced and mapped in a GIS using Adelie Video. The observations were classified following the guidelines of the MSFD Technical Subgroup on Marine Litter for the Mediterranean Sea (Annex 5.1.) (European Commission, 2013). The three classes considered were: Plastic, Metal and Glass/Ceramics. Linear density was calculated using the total length of navigation tracks on each site.

The presence or absence of waste disposal (bauxite residues) at each location was recorded.

2.6 Temporal changes

A qualitative analysis of the temporal changes of *M. oculata* colonies distribution and sizes of the Cassis-200 location was performed. 3D models and images taken in 2017 were compared with video data recorded previously in 2010 (ESSROV 2010) and 2013 (ESSNAUT 2013) (Fabri et al., 2014; Fabri et al., 2017). The videos recorded in 2010 and 2013 did not allow to build 3D-models because they were not recorded for that purpose: the video coverage and image quality were not sufficient, and the submarine navigations were not precise enough. But the 3D-models of 2017 made it possible to precisely identify the scene observed on the videos recorded in 2010 and 2013 and to recognize which knoll and which face of the knoll had been observed at the time. It was therefore possible to choose the orientation of the 3D-model and to compare the same scene at 5 and 7 years apart.

2.7 Validation of the habitat suitability maps built previously

The *in situ* cold-water coral population distribution observed in 2017 was compared to the theoretical distribution obtained from the habitat suitability models (Fabri et al., 2017; Bargain et al., 2018). For this we overlapped both maps in GIS and compared the extent of the distributions. We also gathered all the navigation tracks we were aware of in Cassidaigne canyon (MARUM_2009, MEDSEACAN_2009, ESSROV_2010, ESSNAUT_2013, ESSTECHROV_2017, ESSTECHROVGEN_2017, VIDEOCORI_2017 cruises) in order to map absence of *M. oculata* colonies.

3. Results

3.1 Spatial distribution of the 3D models

A total of 33 models were built in 3D; 10 at Cassis-500, 10 at Cassis-200, 9 on the SW Flank and 4 at the Wall (Fig. 2).

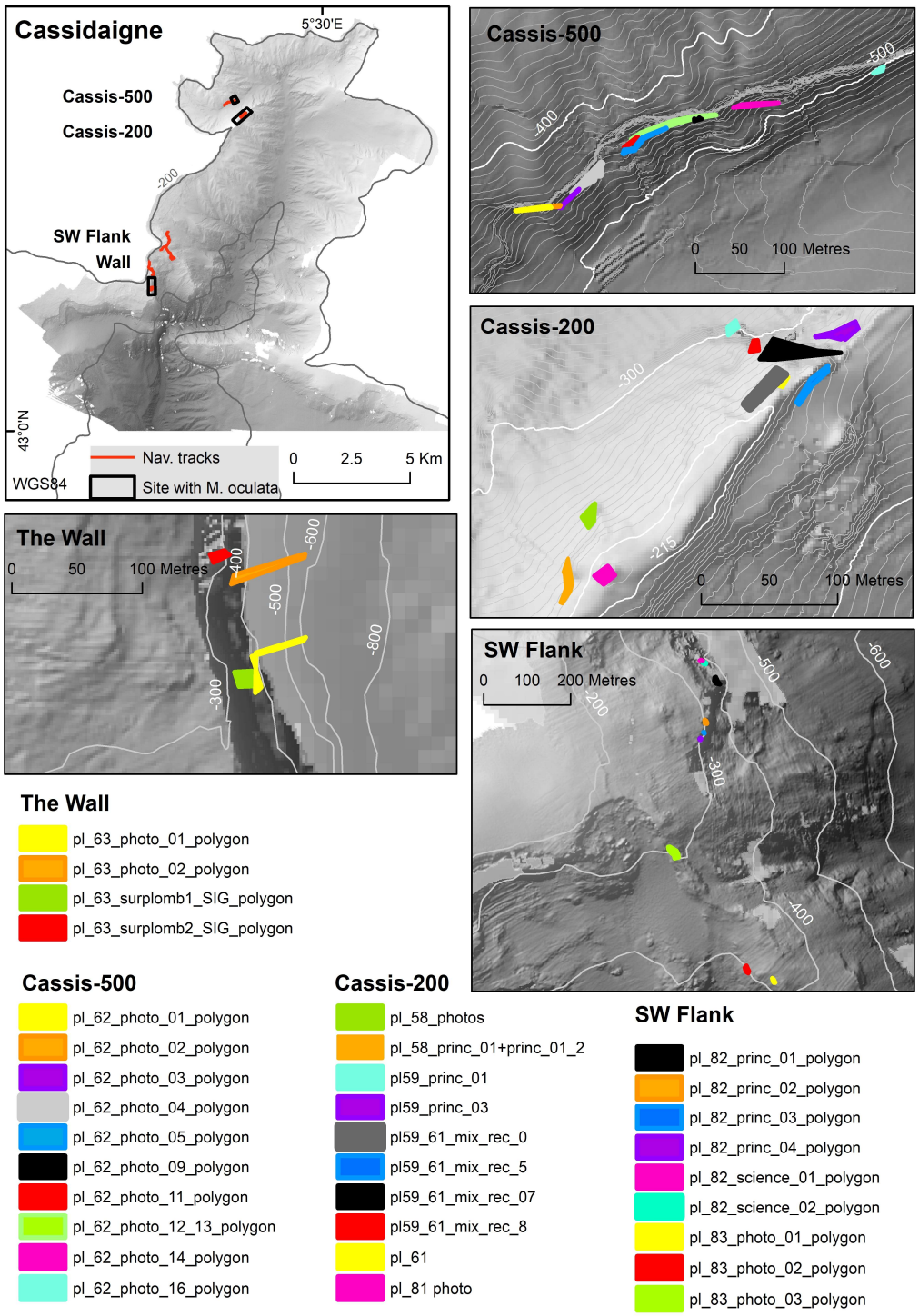

Figure 2: Spatial distribution of the 33 models built in 3D at Cassidaigne canyon, specifically at Cassis-500 (10 models), Cassis-200 (10 models), SW Flank (9 models) and the Wall (4 models). High-resolution bathymetry at each site was collected during the Bathycor Cruise (2016). See supp.mat. B for an exhaustive view of 3D-models.

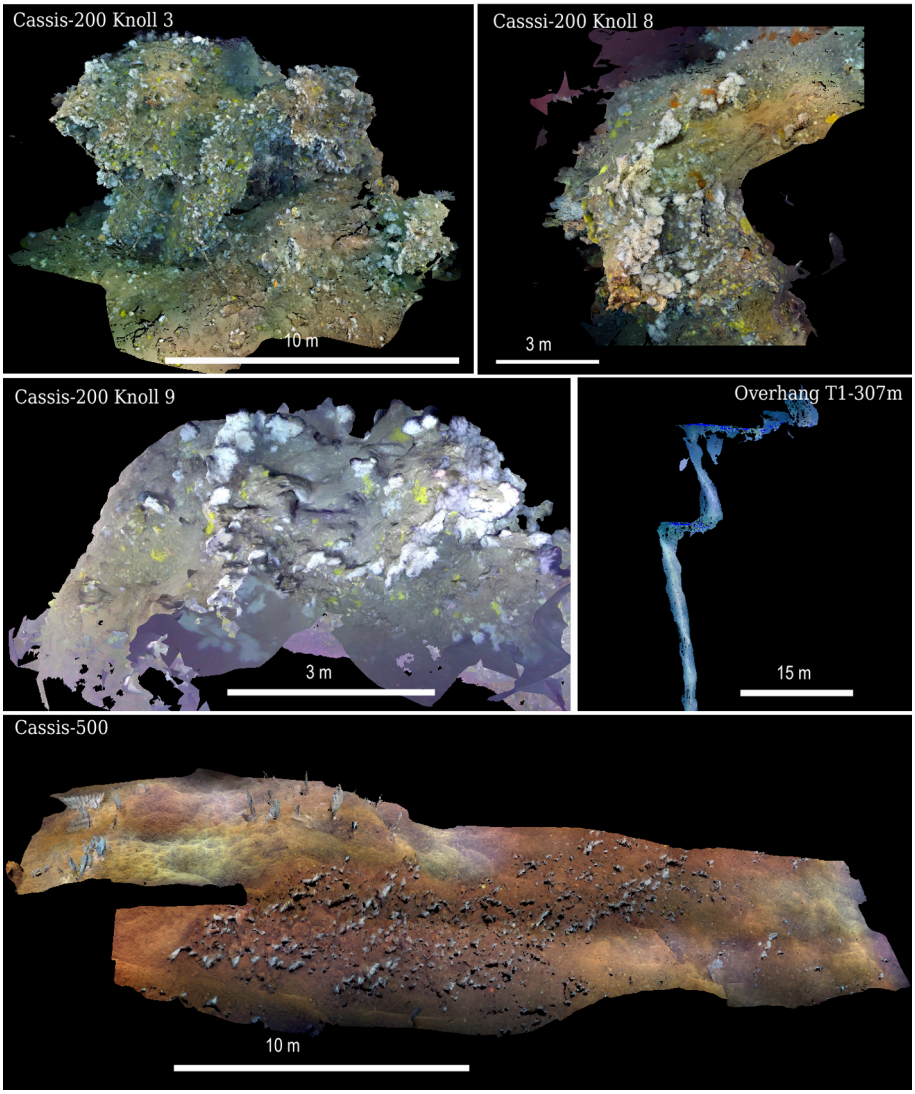

Figure 3: Examples of 3D-models of selected areas within Cassidaigne canyon. See supp.mat B for an exhaustive view of all the 3D-models constructed.

3.2 Scleractinian *Madrepora oculata*

3.2.1 *S*patial and vertical distribution of *M. oculata*

The presence of *M. oculata* was observed in high abundance at three locations: Cassis-500, Cassis-200 and the Wall; but only three colonies were observed at the SW Flank. The vertical distribution ranged from depths of 203 to 484 m.

At the head of Cassidaigne canyon, at Cassis-200, 1294 colonies of *M. oculata* were counted from the 3D reconstructions. Colonies have settled on particular rocky elevations of the area that we called knolls (Fig. 3). We identified a total of 13 knolls where the presence of *M. oculata* was mapped (Fig. 4). Only a few isolated colonies were found in areas in between the knolls. Video observations also showed the presence of colonies on Knoll 13, however no 3D model could be built for this knoll because the video coverage we had was not enough. One knoll was also found with no *M. oculata* (Knoll 4 on the eastern side of Cassis-200), and one knoll (Knoll 12 on the northern side of Cassis-200) was not explored but was identified with the help of bathymetry. This means that at Cassis-200, *M. oculata* was present on a total of 14 knolls, different in size and structure (supp. mat.B). Colonies of *M. oculata* occupied a 3-dimensional spread distribution on each knoll, presenting a south-westerly orientation, facing the dominant currents of the area. Here, the mean depth for the presence of the species was 217±14 m. Because of the patchy distribution of *M. oculata* on the knolls, the vertical distribution on each knoll is presented (Fig. 4). Knoll 3 is the shallowest one, with a mean depth of 206±2 m, ranging from 203 to 211 m. Knoll 5 is the deepest one, with a mean depth of 271±2 m, ranging from 269 to 276 m.

At Cassis-500, also located at the canyon's head, a total of 3492 colonies of *M. oculata* were plotted. The linear exploration performed at this site showed that colonies have settled on the vertical part of a rocky ledge, occupying the whole structure explored (Fig. 4). The entire area was covered by red sediment, and it is important to note that the basal part of tall colonies was covered by red mud. Very small colonies were also seen under overhangs, with no red mud. The deepest observation for the presence of *M. oculata* in the canyon was registered at this site, where colonies were found at a mean depth of 432±10 m, ranging from 416 m to 484 m (Fig.4).

At SW Flank, located at the exit of Cassidaigne canyon, only three colonies of *M. oculata* were observed at the top of a rocky structure, at a depth of 351 m (Fig. 4).

The Wall, a long escarpment also located at the exit of the canyon, was surveyed through two vertical transects of approximately 300 m in height (T1 and T2) (Fig. 5; supp.mat. B). This location was very difficult to explore due to the technical challenge of navigating in this environment below an overhang, something that had never been done before since the tilt cameras of ROVs generally cannot be directed upwards. In this study, it was possible to build 3D models based on video since the part under the overhang was filmed when the H-ROV Ariane accidently bumped the ceiling; however, no photos could be taken. These 3D models allowed showing the complexity of this site where colonies have settled. Along the first transect (T1), two overhangs at different depths (Overhang T1-307 m and Overhang T1-320 m) were found with the presence of *M. oculata* (Fig. 5), whereas a third overhang was found (Overhang T2-340m) along transect 2 (T2), at a deeper part of the wall (Fig. 5). At the Wall, *M. oculata* exclusively colonized the area under the overhangs, with colonies having an upside-down orientation. Around 3000 small colonies were counted under the

three overhangs (only 677 colonies were plotted on the 3D models) and they occupied the entire area. At the Wall (n=677), the mean depth where colonies could be found was 322±15 m. Since colonies had settled under the overhangs, their vertical distribution corresponded to the depth ranges of the latter. Therefore, the shallowest overhang was found between a depth of 305 and 307 m, whereas, just below, the second overhang was found at depths from 323 to 325 m. The deepest occurrence of *M. oculata* at the location was recorded under the third overhang, with a depth distribution that ranged from 339 to 345 m.

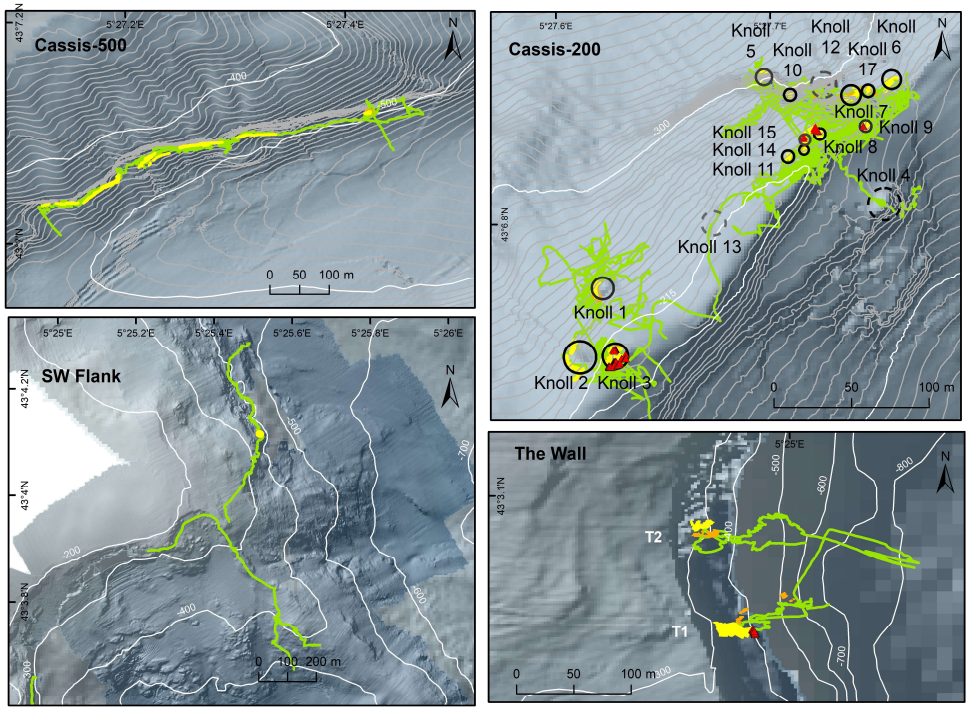

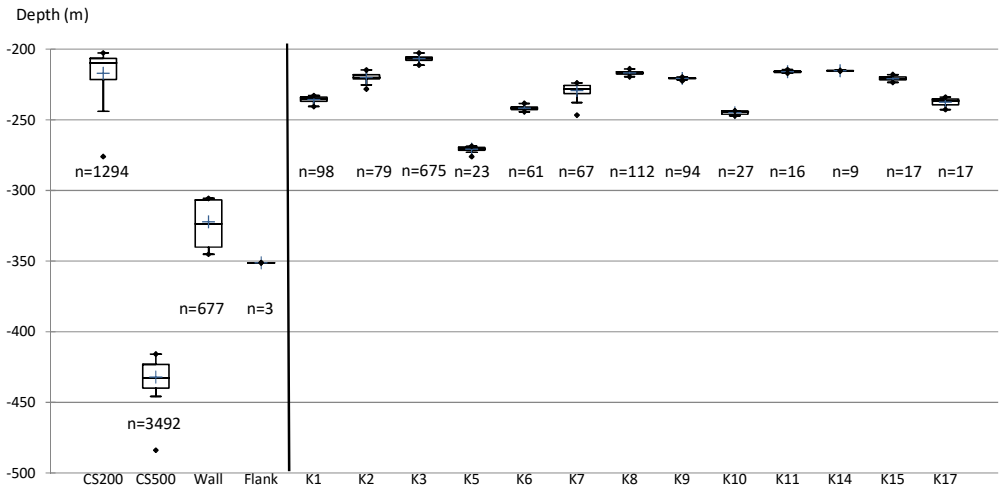

Figure 4: Spatial and vertical distribution of *M. oculata* and *C. rubrum*. Maps show the distribution of *M. oculata* colonies in yellow, rubble in orange, *C. rubrum* colonies in red. Dive navigation tracks are represented as green lines. The graph shows depth-range box-plots of *M. oculata* in Cassidaigne canyon, for each location (Cassis-200, Cassis-500, the Wall and SW Flank) and the detail for each knoll at Cassis-200 (K1 to K17). The number of plotted colonies is indicated on the graph (n) for each location and knoll.

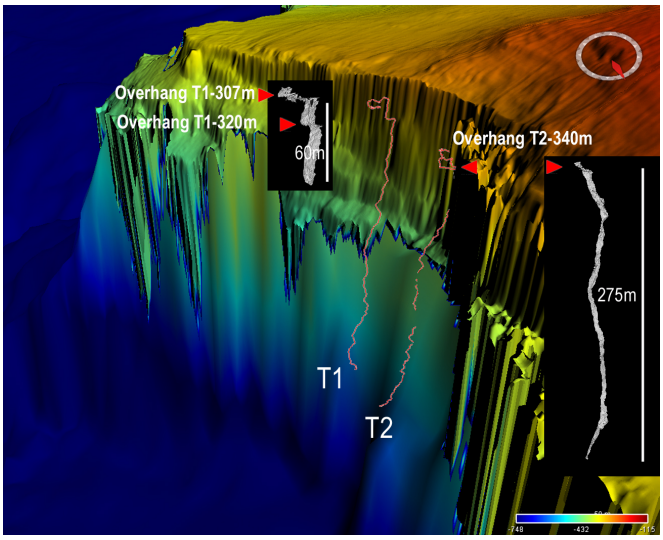

Figure 5: 3D-Representation of the Wall, with the two vertical navigation tracks T1 and T2 and the position of the 3 overhangs located at different depths, where 3D models were made.

3.2.2 Surface coverage and colony density of *M. oculata*

At Cassis-200, the total surface occupied by colonies was 409 m² on the 3D models, and was half as much when transferred into GIS and seen in plan view (Table I). Colonies of *M. oculata* occupied different surfaces and presented different densities depending on the knoll. The largest surface occupied by colonies was seen for Knolls 2 and 3 (Table I). The highest density was found on Knoll 8, with 12 colonies.m^{-2} calculated on the 3D model. Overall, at Cassis-200, the mean density of *M. oculata* calculated in 3D was 4 colonies.m^{-2}.

At Cassis-500, the surface occupied by *M. oculata* was 924 m² on the 3D models, and less than half when transferred into a GIS. The mean density was 4 colonies.m^{-2} in 3D.

Under the overhangs of the Wall, colonies occupied a total surface area of 317 m² measured on the 3D models, which was almost the same when transferred into a GIS because the colonies occupied a horizontal plane under the overhangs, allowing good representation in 2D. At the Wall, the mean density was 9 colonies.m^{-2}, the highest mean density of *M. oculata* in Cassidaigne canyon.

At SW Flank, no estimation of surface/density was calculated since only three colonies were observed.

383

384 **Table I.** Surface coverage and colony density, in 2D and in 3D, for *M. oculata* at Cassis-200, Cassis-500 and the Wall. For the
385 location Cassis-200, the surface and density are presented for each knoll. Total surface and mean densities were calculated for
386 the 3 locations.
387

Location	Knoll	Surface 2D (m^2)	Surface 3D (m^2)	n	Density 2D (nb colonies.m^{-2})	Density 3D (nb colonies.m^{-2})
Cassis-200	Knoll 1	19	38	98	5	3
Cassis-200	Knoll 2	44	104	79	2	1
Cassis-200	Knoll 3	49	101	98	14	7
Cassis-200	Knoll 5	8	42	23	3	1
Cassis-200	Knoll 6	14	32	60	4	2
Cassis-200	Knoll 7	17	30	67	4	2
Cassis-200	Knoll 8	8	9	98	14	12
Cassis-200	Knoll 9	11	14	94	8	7
Cassis-200	Knoll 10	6	6	27	5	5
Cassis-200	Knoll 11	5	5	16	3	3
Cassis-200	Knoll 14	2	2	9	4	4
Cassis-200	Knoll 15	9	11	17	2	2
Cassis-200	Knoll 17	2	3	17	8	7
Cassis-200		200	409	1388	6	4
Cassis-500 SW Flank		409	924	3492 2	9	4
Wall		322	317	677	9	9

388

389

390

3.2.3 Size structure of *M. oculata* populations

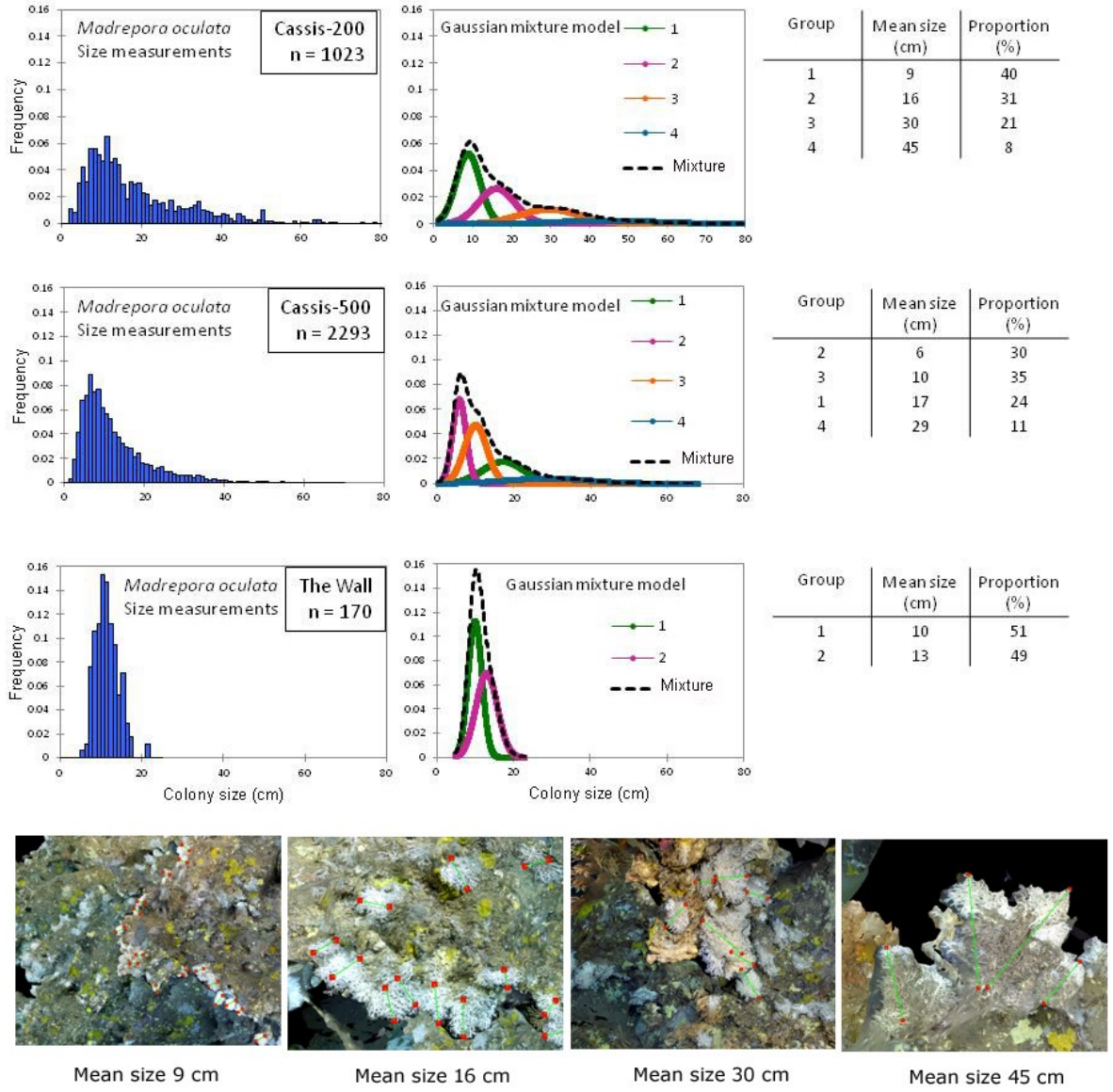

Figure. 6: Histograms of size distribution for *M. oculata* populations at Cassis-200, Cassis-500 and the Wall, and the Gaussian mixture models implemented to identify size groups. Illustration of size measurement on the 3D models for *M. oculata* at Cassis-200 (green line between two red dots).

At Cassis-200, the mean height of *M. oculata* was 18±12 cm (n=1023). Size measurements show colonies as small as 2 cm (smaller colonies were not plotted), while the tallest colony measured 78 cm. The Gaussian mixture model (Fig. 6) shows a size structure of colonies composed of 4 distinct size groups. At Cassis-200, 40% of the colonies were included in the group with the smallest mean size of 9 cm (group 1), whereas 8% of the colonies were included in the largest size group of 45 cm (group 4). At this location, 52% of the colonies were therefore included in intermediate size groups, with 31% of the colonies included in group 2, with a mean size of 16 cm, and 21% included in group 3, with a mean size of 30 cm.

At Cassis-500, the size measurements (n=2293) show that the smallest colony measured 1 cm and the tallest 67 cm, the mean size was 12±8 cm. The Gaussian mixture model for Cassis-500 (Fig. 6) shows that colonies of *M. oculata* belong to 4 different size groups. At Cassis-500, there are therefore 2 groups (groups 2 and 3) in which the smallest colonies were included, with a mean size of 6 and 10 cm, which accounted for 30% and 35% of the colonies, respectively. The model also shows that 24% of colonies of *M. oculata* belong to a group in which the mean size was 17 cm and 11% of the colonies fit in the group in which the mean size observed was 29 cm. Therefore, the results presented by the model indicated that at Cassis-500 a larger part of the population is included in the smaller size groups (with 65% in group 2 and 3) than in the taller size groups (35% in group 1 and 4).

At the Wall, the size measurements (n=170) show colonies with a minimum size of 6 cm and a maximum of 22 cm, and with a mean size of 11±3 cm. The low number of size measurements is due to the low image resolution of the 3D reconstructions made from video for this location. However, the Gaussian mixture model analysis could be performed (Fig. 6). The model suggests that the colonies of *M. oculata* belong to two size groups, with 51% of the colonies included in a group with a mean size of 10 cm and the other 49% included in a group with a mean size of 13 cm.

The Kruskal-Wallis test performed to compare the mean size of *M. oculata* populations on the three locations shows that they are all different. The mean size of *M. oculata* in Cassidaigne canyon was significantly different between Cassis-200 (18±12 cm), Cassis-500 (12±8 cm) and the Wall (11±3 cm) (p-value ≤ 0.05). The global mean size of *M. oculata* in the Cassidaigne canyon was 14±10 cm.

3.3 Forests and gardens of antipatharians

3.3.1 Spatial and vertical distribution of antipatharians

Three antipatharian species, *A. dichotoma*, *A. subpinnata* and *L. glaberrima,* were observed at Cassidaigne canyon. The species *A. subpinnata* was found only at Cassis-200. The two species, *A. dichotoma* and *L. glaberrima,* were found at both Cassis-200 and at SW Flank, while at Cassis-500 only one antipatharian colony was observed, *A. dichotoma,* and no antipatharian was observed at the Wall (Fig. 7).

The distribution of *A. subpinnata* was limited to Cassis-200 at a mean depth of 210±8 m (Fig. 7), where two dense forests of the species were seen at the tops of knoll 3 and knoll 9.

Gardens of *L. glaberrima*, on the contrary, presented a much more widespread distribution, with the presence of the species at both Cassis-200 and the SW Flank, with a depth distribution ranging from 200 to 376 m (Fig. 7). At Cassis-200 (n=124), *L. glaberrima* was observed settled on the side of knolls, as well as between knolls as part of coral gardens at a mean depth of 225±14 m. At the SW Flank (n=21), colonies of this species were observed only in the northern part of the site where *L. glaberrima* occupied the sides of a rocky structure at a mean depth of 322±37 m and dense colonies of *V. flagellum* were observed at the top. Colonies of *L. glaberrima* could be observed either as white or orange. Both morphs could be observed with no link with the size of the colony or its location.

Colonies of *A. dichotoma* was always observed as isolated colonies from 209 to 435 m (Fig. 7) at Casssis-200, SW Flank and Cassis-500.

Colonies of *L. glaberrima* and *A. dichotoma* presented a more extended vertical distribution than the forest forming species *A. subpinnata* (Fig. 7).

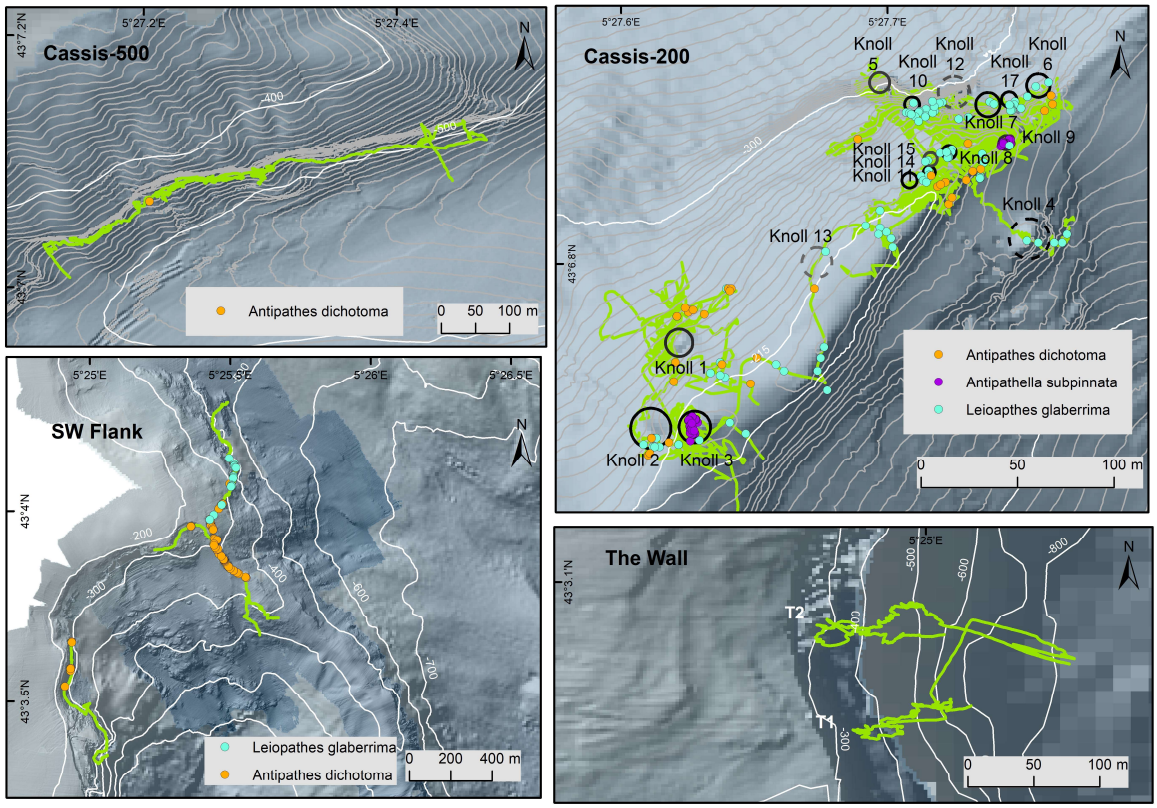

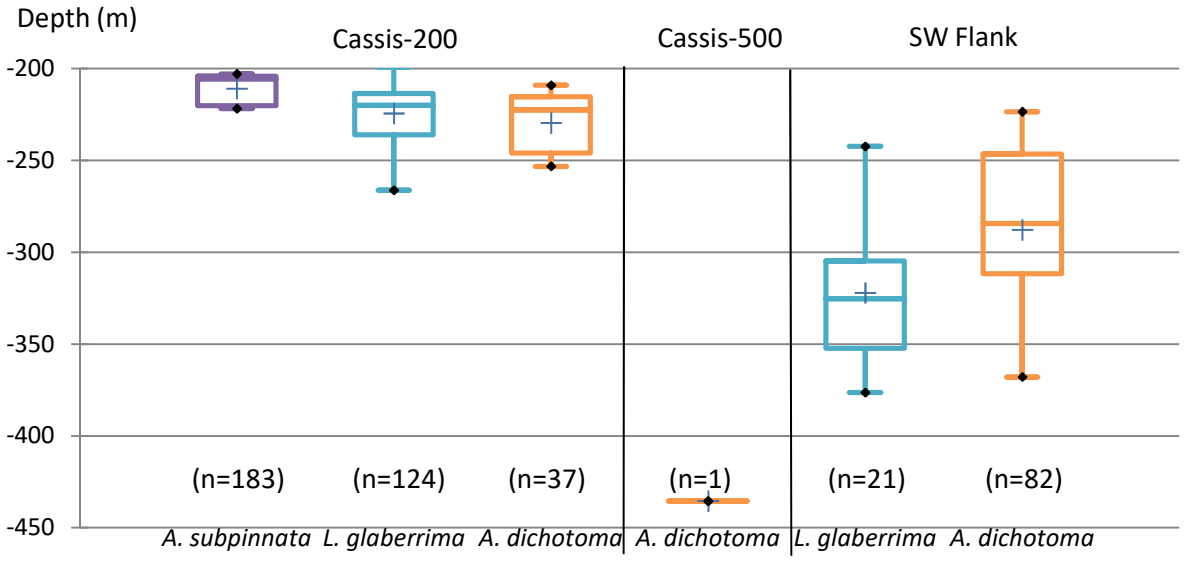

Figure 7: Spatial and vertical distribution of antipatharian species in the Cassidaigne canyon. Maps show the distribution of forests of *A. subpinata* (violin), gardens of *L. glaberrima* (blue), and isolated colonies of *A. dichotoma* (orange). The graph shows depth range box-plots of the three species observed at each location during the Videocorl cruise. No antipatharian was found at the Wall. The number of plotted colonies is indicated on the graph (n) for each species.

3.3.2 Size measurements of antipatharian populations

It was not possible to identify antipatharians on the 3D models due to their movement with the water flow. Hence, it was not possible to perform any size measurements for this group of corals. Nevertheless, a qualitative description of the size structure of the populations was possible based on video and photo analysis (Fig. 8).

At both locations, Cassis-200 and SW Flank, size seemed to be similar among colonies of *A. dichotoma* and no small colonies could be observed (Fig. 8A & 8B).

At Cassis-200, forests of *A. subpinnata* included large colonies occupying the top of two knolls but small colonies had also settled on the sides of knoll 3 (Fig. 8C), whereas no *A. subpinnata* was observed at SW Flank (Fig. 8D).

Colonies of *L. glaberrima* of different sizes were observed at both Cassis-200 and SW Flank. Large colonies of the species could be observed, in particular occupying the sides of knolls at Cassis-200 (Fig. 9E) and vertical walls at SW Flank (Fig. 8F). However, small and intermediate size colonies were also observed in high density, forming coral gardens (Fig. 8G). A mix of small and large colonies was also found at the site SW Flank (Fig. 8H).

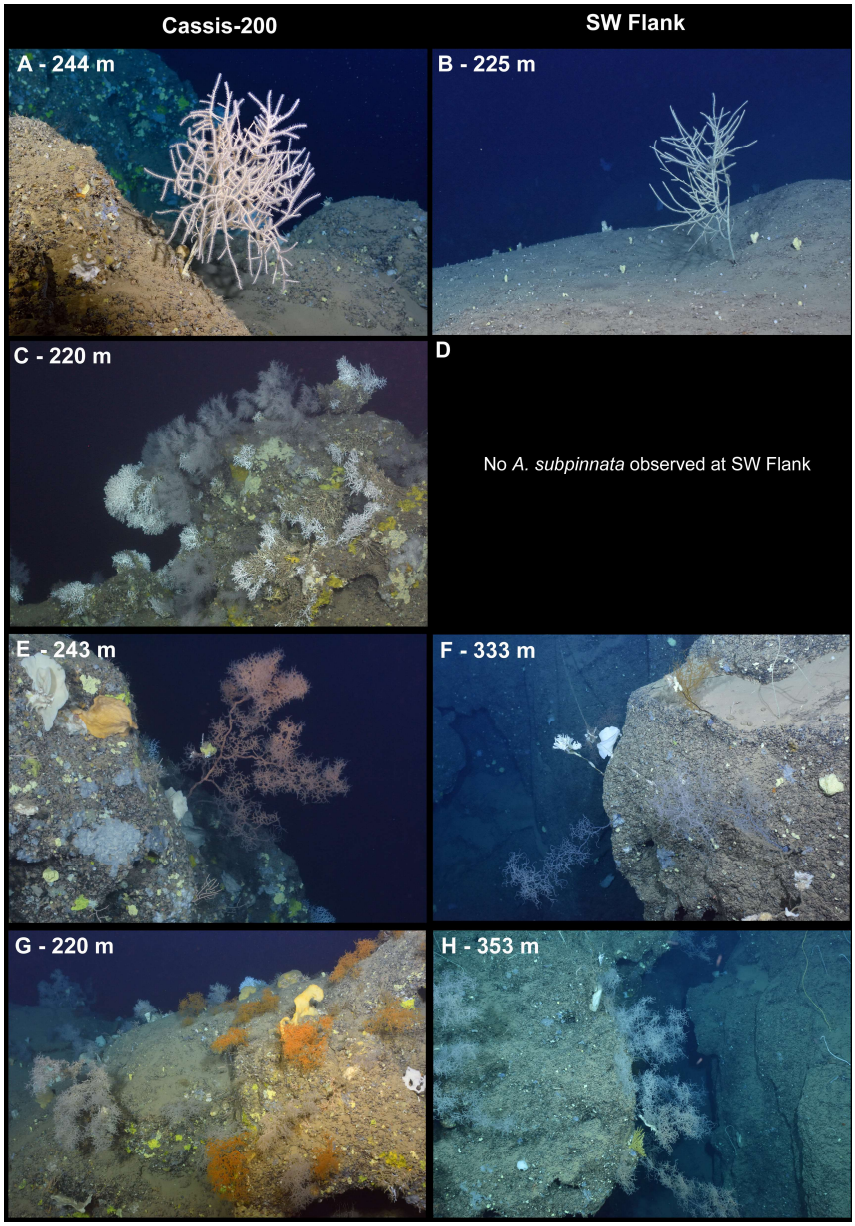

473

474 Figure 8: Qualitative size description of antipatharians from Cassis-200 and SW Flank sites. A and B: Large isolated colonies of *A.*
475 *dichotoma*; C and D: Forest of large colonies of *A. subpinnata* with small colonies around; E and F: Large colonies of *L. glaberrima*;
476 G: Gardens of *L. glaberrima* with colonies of different sizes; H: Colonies of *L. glaberrima* of different sizes.

477

3.4 The Octocorallia Scleraxonia *Corallium rubrum*

3.4.1 Spatial and vertical distribution of *C. rubrum*

The red coral *C. rubrum* was found at two locations: Cassis-200 and the Wall (Fig. 4).

At Cassis-200 (n=123), the presence of *C. rubrum* could be osberved Knolls 3, 8, 9 and 15 (Fig. 4), which are amongst the shallowest. Here, *C. rubrum* was found at a mean depth of 209±5 m, with a vertical distribution ranging from 203 to 220 m depth (Fig. 9). The use of videos and HD photos was essential to locate small patches of colonies, always underhanging the knolls . On Knoll 3, 94 colonies of *C. rubrum* were counted and plotted, while only 16 colonies were counted on Knoll 8, 9 on Knoll 15 and 4 on Knoll 9. Colonies of *C. rubrum* presented a wide distribution along the entire rocky structure of Knoll 3, while on other knolls colonies were concentrated in a small area (Fig. 4).

At the Wall, a total of 42 colonies of *C. rubrum* were counted at a mean depth of 306±1 m (Fig. 9). Colonies were found to have settled all along the outer edge of the overhang T1-307m. The length of the explored edge was around 10m long. Since the occurrence of the species was limited to the outer edge of the overhang, the observations of red coral varied only between 305 and 307 m depth.

3.4.2 Surface coverage and colony density of *C. rubrum*

At Cassis-200, *C. rubrum* colonies were counted on the 3D models when possible, and this was complemented by counting small colonies on HD photos. The total surface area measured on the 3D models was 11 m² and we counted 123 colonies, which gives a density of 11 colonies.m^{-2}. Colonies of *C. rubrum* covered the largest surface (10 m²) on Knoll 3, and showed the highest density on Knoll 8, where the colonies were all gathered in an area smaller than 1 m².

At the Wall, colonies of *C. rubrum* settled on the horizontal edge of the shallowest overhang. We counted 42 colonies on a surface area of 2 m², corresponding to a density of 20 colonies.m^{-2}. Since the colonies were all aligned along the 10 m long edge, a linear density was calculated, corresponding to 4 colonies.m^{-1}.

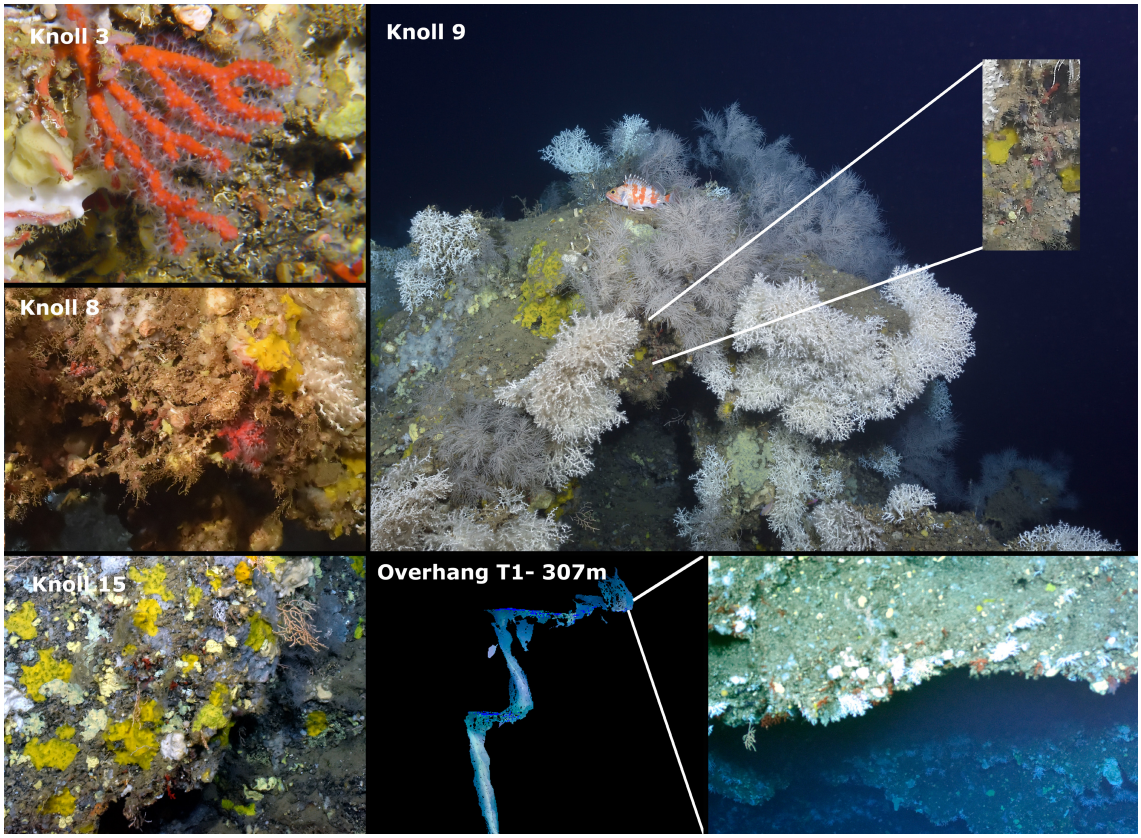

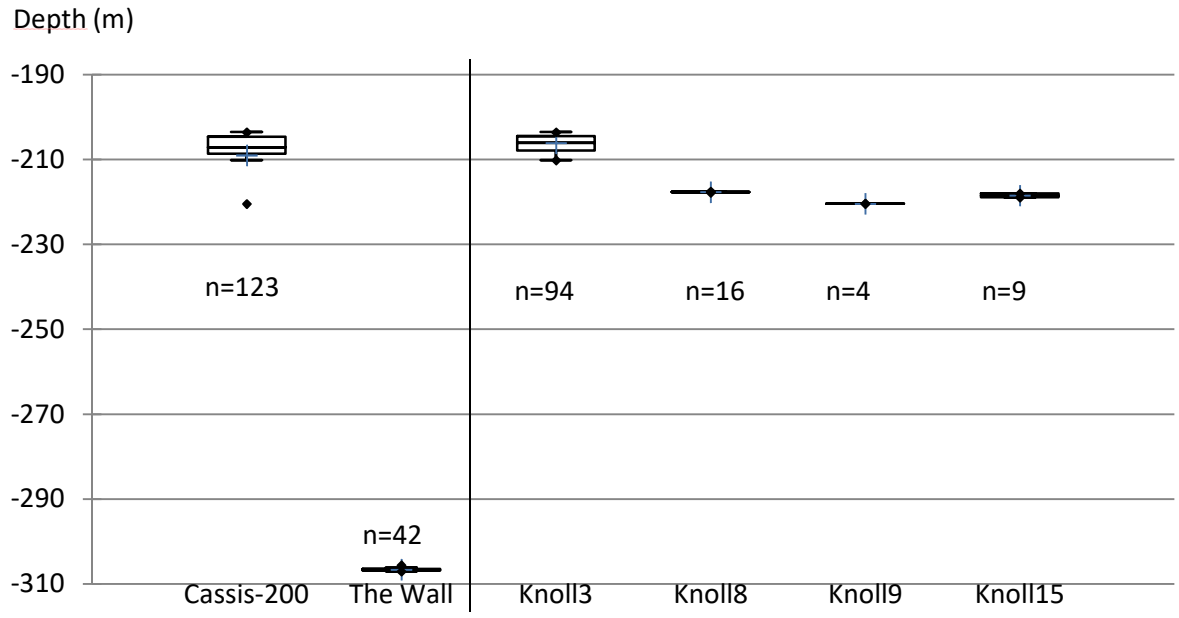

Figure 9. Spatial and vertical distribution of *C. rubrum* in Cassidaigne canyon for each location. Photos show *C. rubrum* in Cassidaigne canyon, at Cassis-200 and the Wall, with close-ups on Knolls 3, 8, 9, 15 and on the ledge of Overhang T1-307m. The graph shows depth-range box-plots of *C. rubrum* in Cassidaigne canyon for each location. The number of plotted colonies is indicated on the graph (n) for each location and knoll.

3.4.3 Size measurements of the *C. rubrum* population

At Cassis-200 on Knoll 3, several size measurements of *C. rubrum* colonies were performed (n=26) on the 3D reconstructions, showing a mean size of 6±1 cm, with the smallest colony measuring 3 cm and the tallest one measuring 16 cm (Fig. 9).

No measurement could be performed on Knolls 8, 9, and 15 because the colonies were too small, or at the Wall, because the 3D models were made with video snapshots, therefore the resolution was not good enough to measure small colonies, although they could be seen on the HD images (Fig. 9).

3.5 Gorgonians *Callogorgia verticillata and Viminella flagellum*

3.5.1 Spatial and vertical distribution of gorgonian populations

Many tall colonies of both gorgonians species were observed at SW Flank while only a few isolated colonies were observed at Cassis-200, and only one species (*C. verticillata*) was observed at Cassis-500 (Fig. 10). Neither of the two species was observed at the Wall.

At SW Flank, dense and tall colonies of *C. verticillata* (n=84) had settled on patches of rocky substrate covered by a thin layer of sediment at a mean depth of 371 ± 19 m (Fig. 10). At this location, dense aggregations of *V. flagellum* (n=234) were also found at a mean depth of 297 ± 45 m (Fig. 10). Linear transects carried out along the edge of the continental shelf have shown its presence almost everywhere. White and yellow-colored *V. flagellum* colonies formed vast forests, settled on rocky substrate.

At Cassis-200, only a few gorgonian colonies were seen at knoll 5 and around knolls in the deepest area. Cassis-200 was the shallowest location where *C. verticillata* (n=6) was observed at a mean depth of 254 ± 17 m, together with *V. flagellum* at a mean depth of 267 ± 17 m (Fig. 10).

At Cassis-500, tall colonies of *C. verticillata* have settled on the top of the ledge previously described, but no *V. flagellum* were observed. At this site, *C. verticillata* (n=57) reached a deeper part of the canyon, at a mean depth of 450±18 m (Fig. 10). The depth range of *C. verticillata* at Cassis-500 varied between 424 and 483 m, being the widest depth range of all the locations, with the highest density recorded at a depth around 430 m.

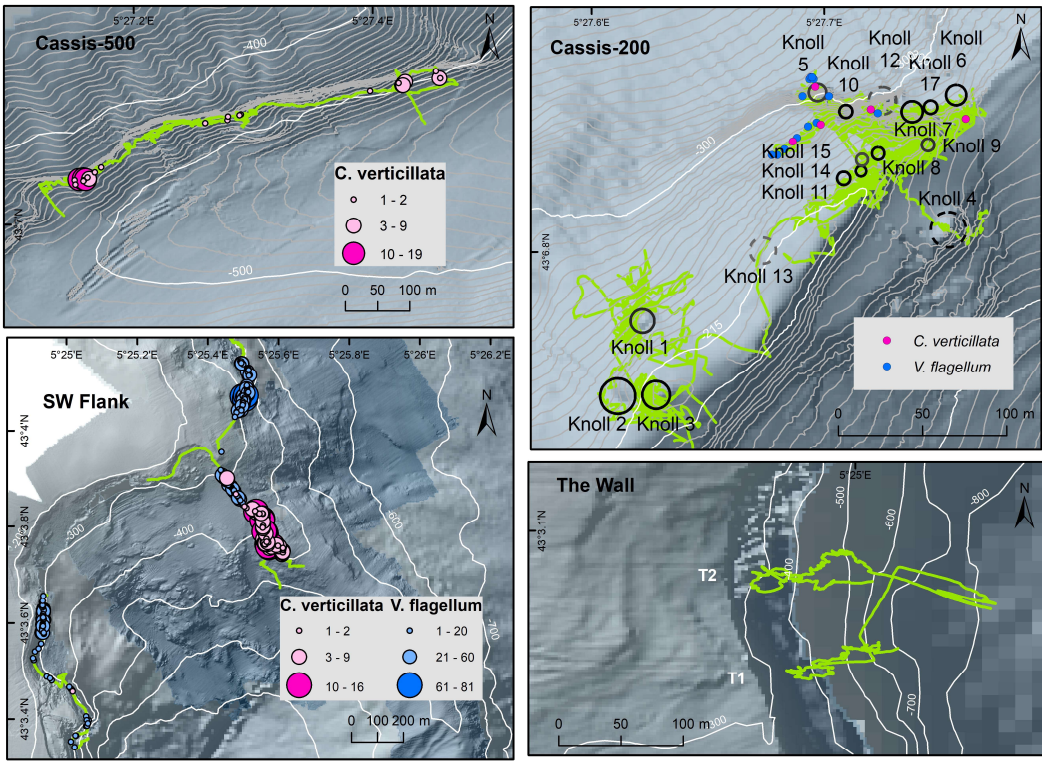

543

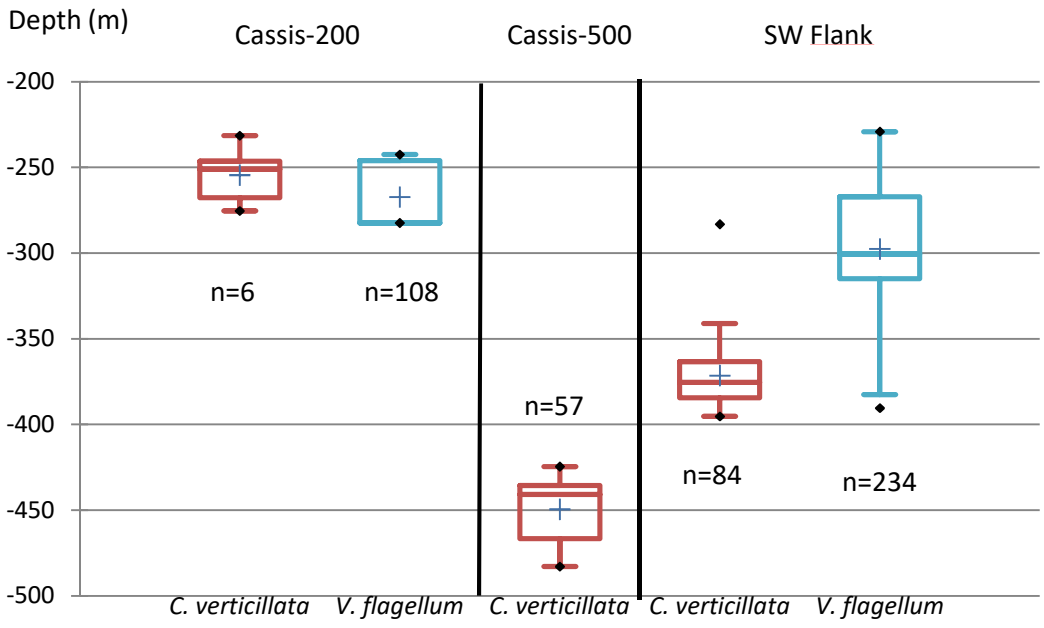

544

545 Figure. 10. Spatial and vertical distribution of the two gorgonian species (*C. verticillata* in red and *V. flagellum* in blue) in
546 Cassidaigne canyon. The number of plotted colonies is indicated on the graph (n) for each species.

547

548

549

550 3.5.2 Surface coverage and density of gorgonian populations

At SW Flank, colonies of *C. verticillata* (437 colonies) were irregularly distributed along a linear transect of 1.2 km. The maximum density estimated was 47 colonies observed along a 20 meter long video transect, corresponding to 2 colonies.m^{-2}. Many more colonies of *V. flagellum* were counted, approximately 3870 colonies irregularly distributed along a linear transect of around 2.2 km in length. The highest density estimated for *V. flagellum* at SW Flank was 316 colonies along a 20 meter long video transect, corresponding to 16 colonies.m^{-1}.

At Cassis-200 on Knoll 5, 24 colonies of *V. flagellum* could be plotted, covering a surface of 7 m^2, corresponding to a density of 4 colonies.m^{-2}., while only 2 small colonies of *C. verticillata* were seen on the same knoll.

At Cassis-500 a total of 104 colonies of *C. verticillata* were counted on videos at the beginning, middle and end of the linear transect of 440 m length. The highest density measured was 19 colonies along two 10-meter video transects, corresponding to 2 colonies.m^{-1}.

3.5.3 Size structure of gorgonian populations

Gorgonian *C. vertillata*

The global mean size of *C. verticillata* in the Cassidaigne canyon was 69 ± 29 cm.

At the SW Flank (n=37), the mean size was 80±27 cm, the smallest colony of *C. verticillata* measured 22 cm and the tallest one measured 144 cm (Fig. 11). The size histogram is bimodal and the result of the Gaussian mixture model shows one group with a mean size of 65 cm (27% of the population) and another group with a mean size of 86 m (73% of the population).

At Cassis-500, size measurements (n=44) show a mean size of 60±28 cm, a minimum size of 18 cm and a maximum size of 109 cm (Fig. 11). The Gaussian mixture model shows three different size groups. The smaller one contains 23% of the population with a mean size of 27 cm, an intermediate group contains 32% of the population with a mean size of 52 cm and the larger group contains almost half of the population (45%) with a mean size of 87 cm.

At Cassis-200, the size of the very few small colonies of *C. verticillata* observed at the periphery of knolls was not measured.

The Mann-Whitney test performed to compare mean sizes of *C. verticillata* colonies at SW Flank and Cassis-500 evidence a difference between the two populations (p-value≤0.05).

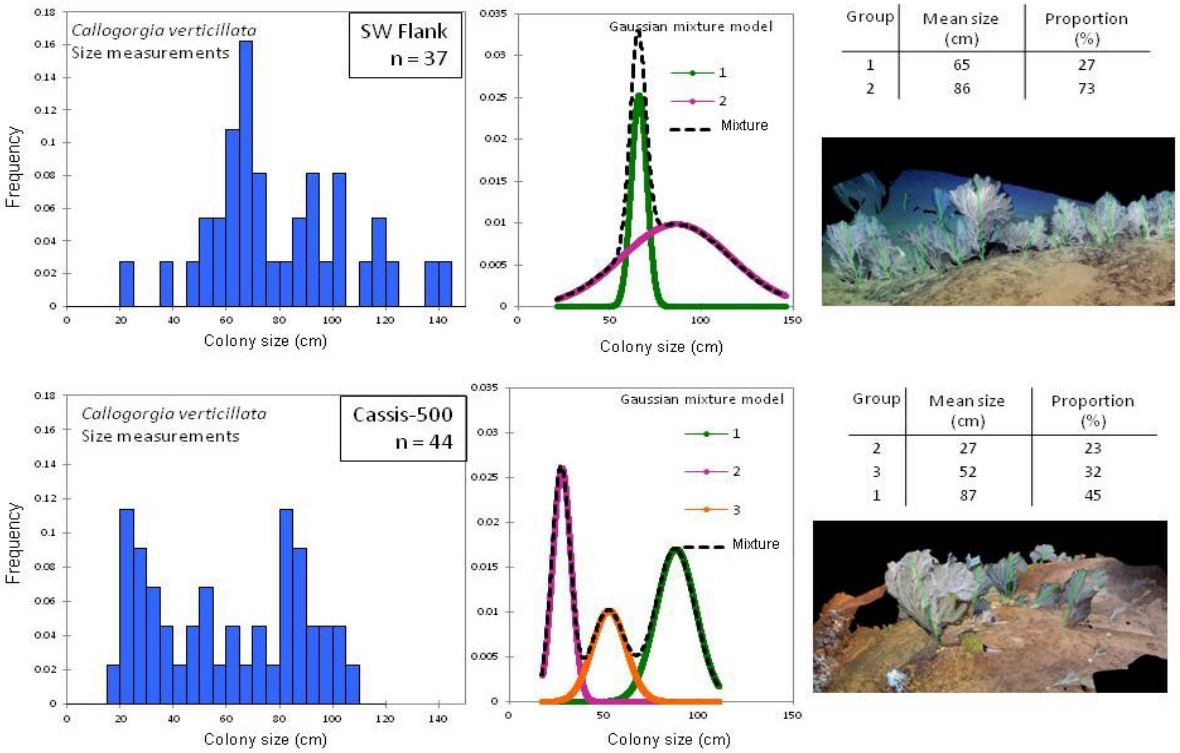

582

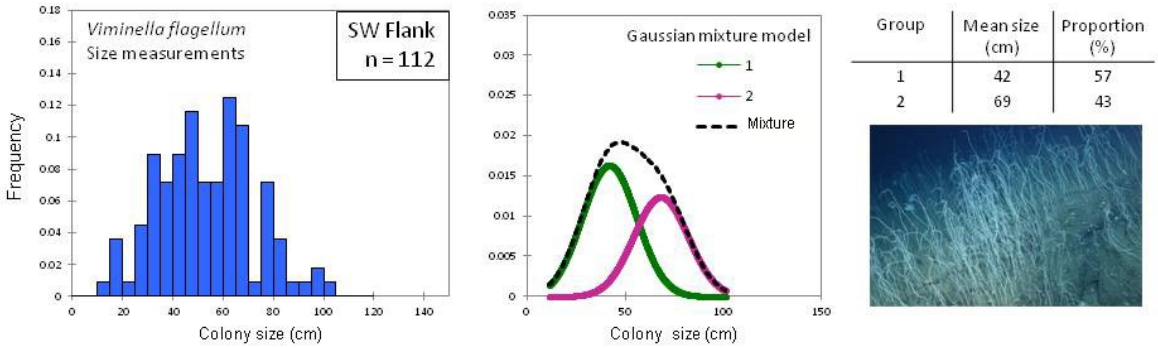

583

584

585 Figure. 11. Histograms of gorgonian size distribution, and gaussian mixture models implemented to identify size groups for *C.*
586 *verticillata* populations at SW Flank and Cassis-500, and for *V. flagellum* population at SW Flank.

587

588

589

590 Gorgonian *V. flagellum*

591 The global mean size of *V. flagellum* in the Cassidaigne canyon was 53 ± 15 cm. Observations showed
592 that most colonies of *V. flagellum* were unbranched, however, when in the presence of one or two
593 branches, the entire colonies measured around 20 cm at most.

594 At SW Flank (n=112), the smallest colony measured 12 cm, while the tallest measured 100 cm. The
595 Gaussian mixture model shows a population composed of two size groups with mean heights of 42
596 cm and 69 cm, with a respective distribution of 57% and 43% (Fig. 11). The overall mean size was 53
597 ± 19 cm.

598 At Cassis-200, only 11 colonies could be measured, and no Gaussian mixture model was computed.
599 The smallest colony measured 39 cm, while the tallest one measured 72 cm; the mean size was 52 ±
600 11 cm.

601 The Mann-Whitney test performed to compare the mean sizes of *V. flagellum* colonies at SW Flank
602 and Cassis-200 locations showed that there is no difference between the two groups. No significant
603 difference (p-value≥0.05) was observed between the mean sizes at Cassis-200 and SW Flank.

604

605 3.6 The diversity of accompanying species

606 In Cassidaigne canyon, the highest species richness was observed at Cassis-200 and SW Flank, with a
607 total of 63 and 52 species of megafauna observed (supp. mat. C). At Cassis-500, we could observe 34
608 different species on photos and videos, while at the Wall only 23 species were observed.

609 Colonies of *M. oculata* were seen at the four locations, and some accompanying species were also
610 present at these locations: the poriferans *Haliclona* (*Haliclona*) *magna*, an encrusting bright yellow
611 sponge (*Hexadella* cf. *crypta)* (Reveillaud et al., 2012) and an encrusting blue gray sponge
612 (*Hamacantha* cf. *falcula*); the scleractinian *Desmophyllum dianthus*; serpulids with calcareous tubes;
613 the decapod *Munida* sp.; the brachiopod *Gryphus vitreus*; the echinoid *Cidaris cidaris*; and the fish
614 *Pagellus bogaraveo*.

615 A minimum of 14 visually distinct sponges could be seen on the photos and videos, but not named
616 because no sampling was performed. Certain others are known from the literature to live in the
617 Cassidaigne canyon and were easily recognized. Therefore, the taxonomic and morphologic list of
618 sponges provided is probably underestimated (supp. mat. C).

619 At Cassis-200, species from the continental shelf could be observed mixed with species from the
620 deep sea, i.e. several colonies of the gorgonian *Paramuricea clavata* (tall and small ones), the
621 decapods *Palinurus elephas* and fish species *Anthias anthias* and *Lapanella fasciata*. The soft coral
622 *Daniela koreni* (pers. Comm. P. Lopez-Gonzales) was also present in high abundance between knolls.

623 The SW Flank is characterized by the dominance of the structuring species *C. verticillata* and *V.*
624 *flagellum.* However, the species composition at this location is similar to what was seen at Cassis-
625 200, in terms of presence/absence but is very different in terms of species abundance and
626 distribution. The analysis of videos and photos showed that *C. verticillata* at SW Flank is a host for
627 several species of epifauna. Species from groups such as zoantharians, sea urchins, hydrozoa,

nudibranchs, crustaceans and ophiuroids were seen occupying the canopy of the alcyonaceans. In most cases, more than one group of epifaunal species was found on a single colony of *C. verticillata.* A total of 44 colonies of *C. verticillata* (out of 437) providing habitat for species of epifauna were observed (10%). Two colonies were found to host the zoantharian *Zibrowius primnoidus* (Carreiro-Silva et al., 2017), 8 Tritoniidae were observed in 8 colonies, and juveniles of Ophiuroidea were found in 17 colonies of *C. verticillata*. Additionally, hydrozoans were found on dead structures. Several individuals (one to four) of the sea urchin *Cidaris cidaris* were found in a total of 7 colonies, most of which were damaged.

The Wall is composed of three different 'habitats' presenting a low diversity of megafauna: the vertical cliff, terraces with coral rubble, and overhangs. Under the overhangs, *M. oculata* was found covering the entire ceiling with a bright blue encrusting sponge between coral colonies. An encrusting pale yellow sponge was also seen on protrusions that resembled fossilized oysters hanging from the ceiling. The outer ledge of the overhang was very rich and harbored many small colonies of the red coral *C. rubrum*, together with *M. oculata*. The vertical cliff was covered by many sponges with *Munida* sp. hidden in small holes of the granular cliff. Terraces serve as repositories for coral rubble falling from the overhangs above. Many skeletons of the scleractinians *Dendrophyllia cornigera* and *M. oculata* were seen on these shelves. Some colonies were still alive as were echinoids probably attracted by the fauna close by.

At Cassis-500, two glass sponges *Farrea bowerbanki* (Boury-Esnault et al., 2017) and cf. *Oospacas minuta* (Bakran-Petricioli et al., 2007) were observed exclusively at this location, in very high abundances. Another glass sponge *Tretodictyum reiswigi* (Boury-Esnault et al., 2017) was also seen in high abundance but was not restricted to Cassis-500. This location is also characterized by the presence of a mixture of small and tall colonies of *C. verticillata*, and only 3 colonies out of 104 (3%) were observed with the presence of epifauna. At this location, the epifaunal groups included one individual of the nudibranch Tritoniidae, a juvenile of the crustacean *Anamathia rissoana*, the zoantharian *Zibrowius primnoidus* (Carreiro-Silva et al., 2017) and a high abundance of juvenile Ophiuroidea. Eggs of an unknown species were also found in the canopy of *C. verticillata* at Cassis-500.

The number of necroses of *C. verticillata* was also registered during video analysis. At Cassis-500, no necroses were found on the 104 colonies of *C. verticillata* however, at the SW Flank, 20 (out of 437) colonies with necroses were observed (4.5 %).

The cluster analysis computed to explore the similarity between the four locations, based on their species composition in presence or absence, grouped Cassis-200 and SW Flank with a Sorensen similarity index above 70%. The Wall was similar to Cassis-200 and SW Flank at 50%, and finally Cassis-500 presented only a 48% similarity to the three other sites (supp. mat. D). The Wall and Cassis-500 harbor different assemblages of species.

666

667 3.7 State of degradation and seafloor integrity

668 3.7.1 Coral rubble of *M. oculata*

669 Coral rubble was found at the three locations where *M. oculata* was present in high abundance,
670 Cassis-200, Cassis-500 and the Wall. The surface occupied by rubble differed between locations
671 (Table II).

672

673 **Table II.** Surface covered by coral rubble, calculated using either a 2-dimension or a 3-dimension approach, for each location
674 where *M. oculata* was observed. The surface covered by coral rubble is also represented in % in relation to the total area
675 occupied by living *M. oculata* at each location (Table I).
676

Location	Rubble 2D (m^2)	Rubble 3D (m^2)	% rubble 2D	% rubble 3D
Cassis-200	68	90	34	22
Cassis-500	9	10	2	1
the Wall	74	154	23	49

677

678

679 At Cassis-200, coral rubble was observed on 9 of the 13 knolls reconstructed in 3D. Rubble was found
680 on the floor under places where colonies have settled. Knoll 3 had the largest surface area covered
681 by coral rubble. Overall, at Cassis-200, coral rubble was measured to cover a surface area of 90 m^2,
682 representing 22% in relation to the total coverage occupied by living colonies.

683 At Cassis-500, coral rubble was only observed in a small area of the site, occupying a surface area of 9
684 m^2 according to the calculations in 2D, and of 10 m^2 according to the calculations in 3D. Coral rubble
685 was found on the floor, under an area covered by living colonies of *M. oculata*, corresponding to 1-
686 2% of their total surface area at Cassis-500. The area where coral rubble was found at Cassis-500 was
687 the only site of the location where images of the seafloor were recorded beneath the ledge colonized
688 by *M. oculata*. Despite the small surface area covered by rubble, Cassis-500 was the only location
689 where dead colonies of *M. oculata* were observed standing in place (see section 3.7.3).

690 The Wall was the site where coral rubble occupied the largest surface area. Coral rubble covered the
691 rugged sections of the vertical wall, just below the overhangs where colonies have settled. The total
692 area occupied by rubble along the Wall was 154 m^2 in 3D, representing 49% of the total surface area
693 observed with living *M. oculata*. When considering the 2D calculations of the surface area, the rubble
694 surface area was 74 m^2, representing 23% of the total area occupied by living *M. oculata*.

695

696 3.7.2 Marine litter

697 A total of 112 litter items were found at the four locations, of which 46 at Cassis-200, 16 at Cassis-
698 500, 41 at SW Flank and 9 at the Wall. The spatial distribution of marine litter observed during video
699 analysis shows the presence of three categories of litter at the four locations in the Cassidaigne

canyon: plastic, metal and glass/ceramics, with a density ranging from 4.9 to 10.6 items.km^{-1} (Table III).

Table III. Distribution of marine litter observation and linear density (item/km) at each location. Sub-categories of plastic have been defined according to the criteria established by the MSFD for the Mediterranean Sea.

		Cassis-200	Cassis-500	SW Flank	Wall
	A2 : bottles	1			
	A5 : other plastic objects	1			
A - PLASTIC	A6 : Fishing nets	0	1	3	2
	A7 : Fishing longlines	44	13	35	6
	A8 : Other fishing related		1	1	1
C -METAL	(beverage can)		1		
D - GLASS	(bottle)			1	
Total nb of item		46	16	40	9
Total navigation length (km)		4.838	2.035	3.775	1.825
Item/km		9.5	7.8	10.6	4.9

Derelict fishing gear (98 longlines and fishing nets) belonging to the plastic category (105 items), was the type of marine litter observed most, as it was found at all four locations (Table III). Entanglement of coral colonies is one of the principal impacts observed at Cassis-200 (see Knoll 3 and 5 in supp. mat. A). Plastic, including fishing gears, was the most abundant category of marine litter found at the Cassidaigne canyon, accounting for 93 % of all litter items. A total of 5 sub-categories of plastic, out of the 10 defined by the MSFD, were found at the Cassidaigne canyon (Table III). Derelict fishing gears were the sub-categories that contributed to the high abundance of plastic along the canyon, with fishing lines (category A7) representing between 67% and 98% of the abundance of plastic marine litter.

3.7.3 Waste disposal

Cassis-500 was the only location where video images showed the presence of bauxite residues. The entire ledge inspected was covered by red sediment (Fig. 12) with living colonies of *M. oculata,* having their basal part covered by red mud. In the deepest part of Cassis-500, colonies of *M. oculata* were seen standing in place but dead and completely covered by red mud (Fig. 12B), showing no existence of a living part at the apex of the colony. Cassis-500 corresponds to a surface area of 924 m² of a total of 1650 m² occupied by *M. oculata* (Table I), which means 56% of the explored *M. oculata* habitat is impacted by bauxite residues in the Cassidaigne canyon.

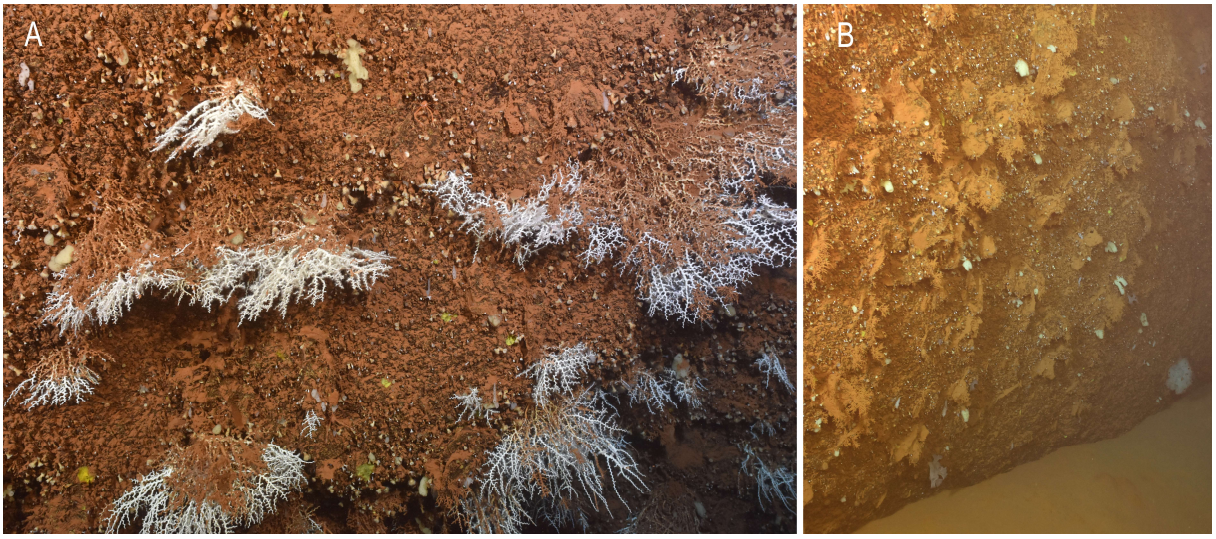

Figure 12. Colonies of *M. oculata* impacted by the disposal of bauxite residues at Cassis-500: (A) The basal part of living colonies covered by red mud and (B) a vertical wall covered with dead colonies.

3.8 Temporal changes at Cassis-200

Two knolls (Knoll 3 and 9), easily identifiable at the location Cassis-200 on the 3D reconstructions, were recognized in the video footage recorded previously in 2010 and 2013.

Photos of Knoll 3 were taken with an interval of seven years (2010 and 2017), while photos of Knoll 9 were taken with one of five years (2013 and 2017) (Fig. 13). The corresponding 3D reconstructions were built and helped the recognition of both knolls (Fig. 13).

At Knoll 3, no major differences could be seen between 2010 and 2017. However, possible growth in the size of colonies and the establishment of two new colonies could be observed, although the videos from 2010 were of poor quality and no HD images were taken (Fig. 13). At Knoll 3, a fishing long line seen in the 3D reconstruction of 2017 was also seen during the analysis of the video of 2010, showing its persistence over seven years.

At Knoll 9, no major differences could be seen between 2013 and 2017. Only apparent growth was noted for *M. oculata* colonies (Fig. 13). However, no big differences in the sizes of the rest of the *M. oculata* colonies were observed.

However, videos from 2010 and 2013 were not dedicated to *M. oculata* observation, and no HD images were taken and no 3D models were built at those times, therefore differences could not be quantified and these results should be interpreted with caution.

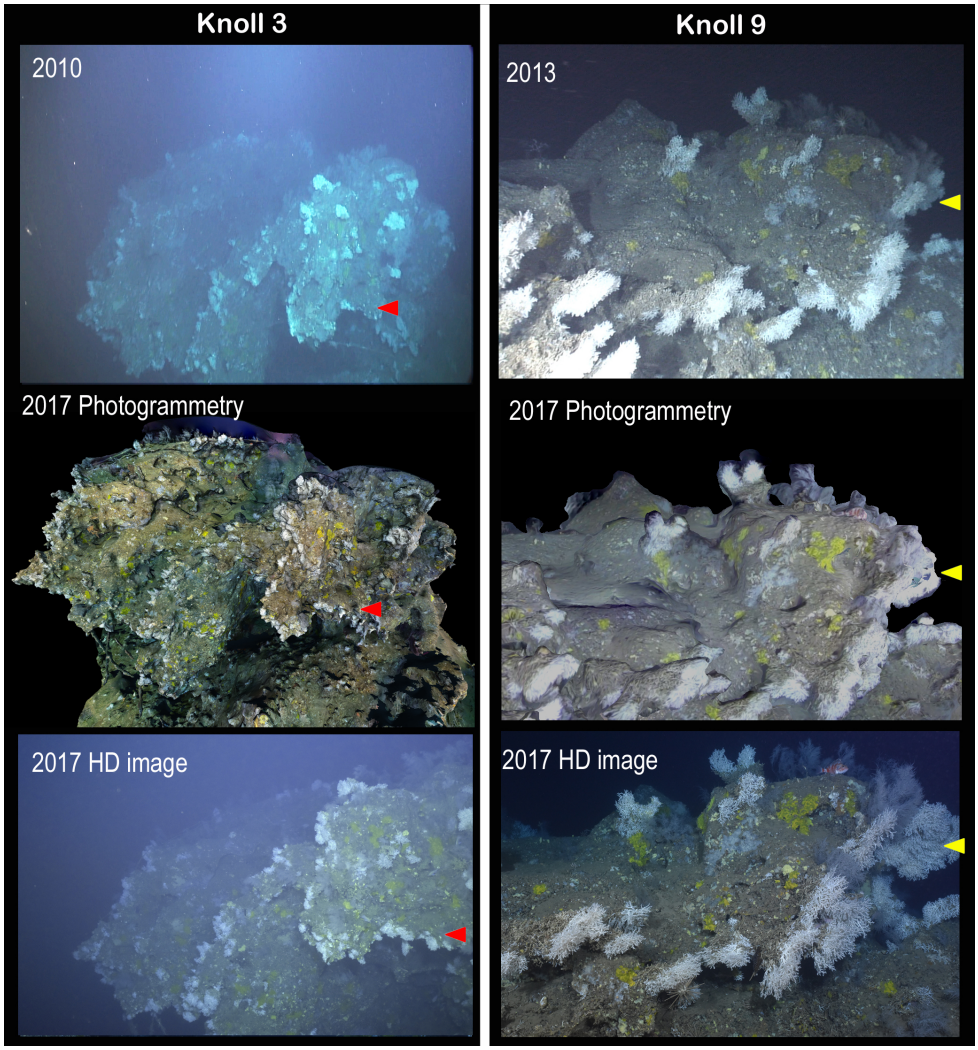

Figure 13: Illustration of the temporal changes at Cassis-200. Photos and 3D reconstruction of Knoll 3 at seven years interval, the arrows indicate the place where two new colonies could be observed in 2017 compared to 2010, and Knoll 9 at five years interval, yellow arrows indicate the colonies that seem to have grown in 2017 compared to 2013.

3.9 Validation of the habitat suitability model built previously

The inspection of Cassidaigne canyon in 2017 was driven by the habitat suitability maps built previously (Fabri et al., 2017; Bargain et al., 2018). However, not all the locations highlighted as suitable by the model could be explored, especially that located on the eastern flank (Fig. 14). But the exploration of Cassis-200, Cassis-500 and the Wall was a success and revealed a very high concentration of *M. oculata* colonies, as described in this paper. The exploration of the SW Flank did not specifically show *M. oculata* populations, but other cold-water corals, such as gorgonians and antipatharians were observed in high concentrations (Fig. 7, 11 & 15). Distribution of the absence of *M. oculata* colonies is shown by mapping all the navigation tracks in Cassidaigne canyon (Fig. 14). Despite the effort made for the exploration of the eastern flank, no *M. oculata* colony could be found.

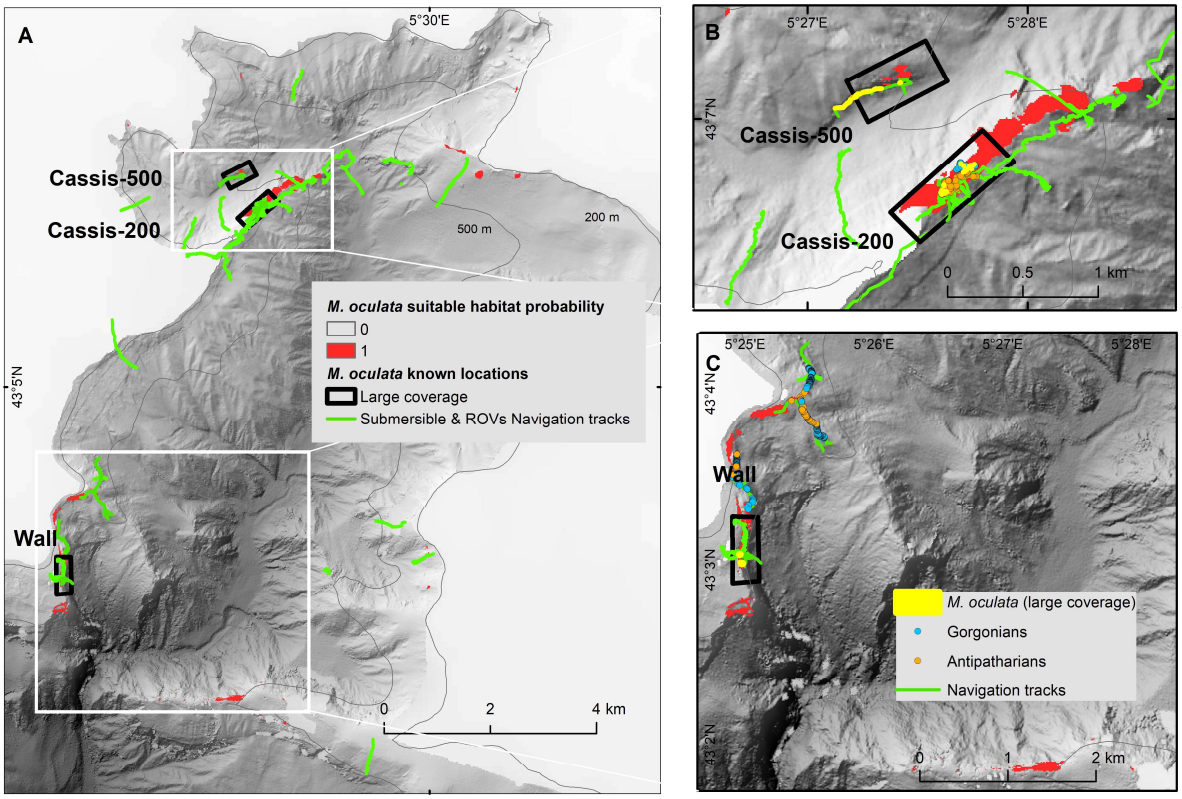

Figure 14. A - Map displaying the probability of the presence of *M. oculata* in Cassidaigne canyon generated with a model built using MaxEnt, from (Fabri et al., 2017), and all submersible and ROVs navigation tracks we could gather (cruises MARUM_2009, MEDSEACAN_2009, ESSROV_2010, ESSNAUT_2013, ESSTECHROV_2017, ESSTECHROVGEN_2017, VIDEOCORI_2017). B and C: Probability of presence of *M. oculata* in red, Navigation tracks in green and *in situ* observation of different species of cold-water corals from Videocori, *M. oculata* in yellow, gorgonians in blue, antipatharians in orange.

4. Discussion

4.1 Spatial and vertical distribution

In our study *M. oculata* was seen to occupy a vertical distribution at depths ranging from 203 to 483 m. At Cassis-200, colonies of *M. oculata* were found on 14 knolls (including Knoll 13 where no 3D model was built). The mean depth of occurrence of *M. oculata* was 215±14 m. In other parts of the Gulf of Lion they were found as shallow as 129 m depth in the La Fonera canyon, but most frequently between 180 and 300 m (Lastras et al., 2016). At Cassis-500, colonies of *M. oculata* settled on the vertical part of a deep (432±10 m) and long (circa 400 m) rocky ledge, with the lower limit of the observed distribution at 483 m. However, during a previous cruise in 2013, *M. oculata* colonies were observed further east along the rocky ledge, reaching depths of 515 m (Fabri et al., 2017). At the Wall, a vertical cliff more than 300 m high, colonies of *M. oculata* had settled in an upside-down position and in high density under overhangs encountered at different depths (307, 320 and 340 m). Due to the challenging navigation conditions in this complex location, the ROV navigated at a safe distance from the cliff and the footage of the cameras therefore covered a 10-meter wide band. But the overhangs are probably larger than the surveyed area, and colonies of *M. oculata* probably cover a surface area larger than that measured at the Wall during the present work. On the SW flank only three colonies could be plotted at a depth of around 350 m. Two other colonies had already been seen in this area in 2009 but they were located shallower at 324 and 244 m (Fabri et al., 2014). Therefore, we can assume that at this location either colonies are sparsely settled, or that we have not yet found the area of high concentration. The wide depth distribution of *M. oculata* seen in Cassidaigne canyon is probably related to its high tolerance to environmental conditions (Wienberg et al., 2009), making it the most dominant structuring species in the Mediterranean Sea (Freiwald et al., 2009; Gori et al., 2013; Fanelli et al., 2017), whereas in the North Atlantic scleractinian structuring ecosystems are mainly composed of *L. pertusa* (Roberts et al., 2003; Costello et al., 2005; van den Beld et al., 2017).

Forests of *A. subpinnata* were observed on the top of two knolls at Cassis-200, at depths of 203 m (Knoll 3) and 220 m (Knoll 9). Colonies were grouped together, surrounded by *M. oculata* colonies. In the Mediterranean Sea, the depth distribution of *A. subpinnata* is often reported to be between 60 to 100 m deep (Bo et al., 2009); however, around Malta, this species was observed between 250 to 400 m (Deidun et al., 2015; Evans et al., 2016). Our observations between these two depth ranges provide new information on the depth distribution of the species, insofar as relatively little is known about this distribution.

Gardens of *L. glaberrima* presented a wider vertical distribution, between 214 and 355 m depth. This is consistent with previous observations commonly reporting the species at depths exceeding 600 m in the Mediterranean Sea (Carlier et al., 2009; Angeletti et al., 2014; Bo et al., 2014; Mytilineou et al., 2014; Angeletti et al., 2015; Bo et al., 2015; Ingrassia et al., 2016). In the Cassidaigne canyon, gardens of *L. glaberrima* were seen in the vicinity of *M. oculata* habitats and also in the vicinity of dense forests of gorgonians *V. flagellum*, something that was also described in Maltese waters (Deidun et al., 2015). Spatial distribution of *L. glaberrima* in the Mediterranean Sea has mainly been highlighted in the eastern part of the western basin (Massi et al., 2018), therefore our records provide new information on its distribution in the western basin.

The antipatharian *A. dichotoma* was observed as isolated colonies at depths from 209 to 435 m, which is consistent with previous records in the Mediterranean Sea reporting the species at depths from 100 to 650 m (Mastrototaro et al., 2010; Bo et al., 2011; Mytilineou et al., 2014; Fourt et al., 2017; Bo et al., 2018).

The precious red coral *C. rubrum* was found at depths between 203 and 307 m in the Cassidaigne canyon. In the NW Mediterranean Sea, red coral presents a very wide vertical distribution, ranging from 16 m (Tsounis et al., 2006) to the deepest record at 1016 m off Malta (Knittweis et al., 2016). We observed *C. rubrum* in association with *M. oculata* ecosystems at two locations (Cassis-200 and the Wall), an association that has already been described in other canyons of the NW Mediterranean Sea such as in the Spanish canyons, Cap de Creus between 50 and 100 m (Rossi et al., 2008) and La Fonera between 100 and 160 m (Lastras et al., 2016).

The fan-forming alcyonacean *C. verticillata* was found at depths between 377 and 483 m at SW Flank, and isolated colonies were also found at a depth of 232 m at Cassis-200. The upper limit of the *C. verticillata* population in the Mediterranean Sea was determined as 120 m (Bo et al., 2012b; Bo et al., 2014; Bo et al., 2015), but its distribution is normally reported to be between 300 and 1000 m deep (Mastrototaro et al., 2010; Deidun et al., 2015), which corresponds to our observations.

The whip gorgonian *V. flagellum* was found forming large forests at depths between 279 and 390 m. This species has often been observed in the Atlantic Ocean (OCEANA, 2011), presenting a vertical distribution from 90 to 1000 m. In the Mediterranean Sea, the species has been documented in Italian waters (Giusti et al., 2012; Angiolillo et al., 2014; Cau et al., 2017; Giusti et al., 2017), and its distribution is known between 90 to 200 m. Our results extend knowledge on the vertical distribution of *V. flagellum* with the report of large forests at water depths down to 390 m.

4. 2 Surface and density

In this study *M. oculata* was seen to cover a global surface of around 1650 m² in the canyon, with 56% of the surface area at Cassis-500, 25% at Cassis-200 and 19% at the Wall. However, we can assume that the surface area is probably larger at the Wall since the overhangs are probably larger than what could be seen. The surface area is also probably larger at Cassis-500 because we had to stop the dive before reaching the end of the ledge, and we know that further east, colonies of *M. oculata* have settled to a depth of 515 m (Fabri et al., 2017). Surface areas are rarely mentioned in the literature because navigation tracks are not usually dedicated to photogrammetry. The highest density of *M. oculata* was 12 colonies.m^{-2} on Knoll 8 at Cassis-200, but colonies were irregularly distributed among knolls and the density was 7 colonies.m^{-2} on Knolls 3 and 9, and even lower on Knolls 2 and 5 (1 colony.m^{-2}). On the contrary, at the Wall colonies were regularly distributed and entirely covered the ceiling of the overhangs, but they were of smaller sizes. The mean densities were 4 colonies.m^{-2} at Cassis-200 and Cassis-500, and 9 colonies.m^{-2} at the Wall. Our results are similar to those found previously in the Cap de Creus canyon where densities of *M. oculata* were calculated to reach a maximum of 11 col.m^{-2}, with a mean density lower than 1 col. m^{-2} (Orejas et al., 2009).

The precious red coral *C. rubrum* was found on areas of 11 m² at Cassis-200 (11 colonies.m^{-2}) and only 2 m², but in higher density (20 colonies.m^{-2}), along the edge on the top of the cliff at the Wall. Red coral was reported in other canyons of the Gulf of Lion, mainly on the upper walls and near vertical walls (Lastras et al., 2016), but no surface areas or densities were calculated.

Forests of gorgonians were not mixed and at SW Flank they were either composed of *C. verticillata* (2 colonies.m^{-1}) or *V. flagellum* (16 colonies.m^{-1}) distributed in patches each around 20 meters long. At Cassis-500 a population of *C. verticillata* had settled on the ledge (2 colonies.m^{-1}) in patches of around 10 meters long, while at Cassis-200 very few colonies were seen and only in the deepest part of the site. On the Montenegrin margin, the gorgonian *C. verticillata* was reported in densities of up to 5 colonies.m^{-2} (Angeletti et al., 2014), which is higher than what we could observe in the Cassidaigne canyon. Around the island of Sardinia and in the Strait of Sicily, *V. flagellum* was reported in densities lower than 0.5 colonies.m^{-2} (Giusti et al., 2017) and up to 60 colonies.m^{-2} (Angiolillo et al., 2014). We only calculated linear densities, but images of *V. flagellum* forests show similar densities in Italian waters as in the Cassidaigne canyon.

4.3 Size structure of populations

At Cassis-200 we could observe the tallest population of *M. oculata*, with the highest colony being 78.3 cm. The structure of the population was composed of four different size groups (mean sizes 9 cm, 16 cm, 30 cm and 45 cm) in which 41% of the colonies are in the group of small specimens, and only 8% are in that of the tallest. A population structure composed of similar size groups (<10cm; 10-20 cm; 20-40 cm and higher than 40 cm) was also described in the Cap de Creus canyon (Gori et al., 2013). The presence of small colonies is described to indicate active recruitment (Gori et al., 2013).

At Cassis-500 the size structure of *M. oculata* population is composed of four groups (mean sizes = 6 cm, 10 cm, 17 cm, 29 cm), in which 65% of the population belong to the two smallest size groups. These mean sizes are smaller than those measured at Cassis-200. We hypothesize that the small size of the population is a consequence of anthropogenic impacts occurring during the last 50 years (Dauvin, 2010; Fontanier et al., 2012; Fontanier et al., 2015; Fabri et al., 2017). The high sedimentation rate of bauxite residues may have prevented *M. oculata'*s growth by suffocation, by starvation or by preventing settlement of new colonies. Colonies were seen only on vertical parts or under the rocky outcrops but not on the top of the ledge where there is probably too much sedimentation for larvae to cope with and settle. According to the minimal growth rate of *M. oculata*, shown to be 3 mm/year (Orejas et al., 2008), the smallest size groups of colonies (mean size = 6 and 10 cm) observed in our study are around 20 and 30 years old. The measurement of the size of the colonies performed in this study supports what was initially hypothesized for this location (Fabri et al., 2017), that is the recruitment of *M. oculata* at Cassis-500 probably occurred after the reduction of red mud discharges in 1988, 30 years ago, due to the termination of production by one of the two main aluminum factories. Since the discharge of particles stopped in January 2016, our measurements performed one year after the end of this pressure can be used as a reference for future measurements dedicated to monitoring this site's recovery.

At the Wall the population of *M. oculata* was composed of small colonies (two groups of mean sizes 10 and 13 cm), in very high density under three overhangs at depths between 307 and 340 m. No

large colonies could be observed, all of them were upside down, and coral rubble was seen to cover terraces below the three overhangs. We can thus assume that colonies fell due to their own weight and because of their downward orientation. Colonies are thus naturally unable to reach large sizes at this location, nor can they be physically impacted by human activities because they are protected by the overhang. This makes the Wall a location that can be considered as a reservoir for the *M. oculata* population in the Cassidaigne canyon, ensuring the persistence of the species, since it can spread to other areas given their reproduction processes based on external fertilization (Freiwald et al., 2009; Pires et al., 2014). However, if colonies keep falling off once they reach a certain size, it is also possible that the population at the Wall itself also relies on recruitment of larvae from elsewhere.

Colonies of *C. rubrum* were very small, with a mean size of 6 cm height and with the tallest colony found measuring 16 cm in Cassidaigne canyon. In other canyons, heights of *C. rubrum* populations were also measured to be small, i.e. in Cap de Creus canyon they hardly reached 6 cm (Rossi et al., 2008) and in La Fonera canyon, *C. rubrum* was reported as small, centimetric colonies (Lastras et al., 2016). The small size of *C. rubrum* colonies has been shown not to be related to depth, but to disturbances occurring in the environment (Cau et al., 2016). Therefore, the small size observed for the *C. rubrum* population in Cassidaigne canyon is probably due to intense hydrodynamic processes occurring in the canyon (Fabri et al., 2017). The water flow generated by upwelling and downwelling phenomena in the canyon could be a disturbance slowing down the colonies growth. Whereas larger colonies can be observed in deeper waters where there are less constraints from the environment, and a more stable temperature (Galli et al., 2016). For example, *C. rubrum* colonies of good size, in view of their many branches, were seen at a depth of 1000 m off Malta (Knittweis et al., 2016).

The height of antipatharian colonies could not be measured because of their flexibility and their movement in the water flow, which prevented photogrammetry. However, it was possible to observe different sizes of both species *A. subpinnata* and *L. glaberrima*, suggesting active recruitment and healthy populations. *Antipathes dichotoma* was always seen in tall colonies and no small ones were reported. This might be because small colonies could not be seen on the videos as they are very thin and flattened against the substrate. Antipatharians are amongst the oldest known marine organisms, with very slow growth and millennial longevities (Roark et al., 2009; Carreiro-Silva et al., 2013). *Leiopathes glaberrima* and accompanying benthic invertebrates have been reported as Vulnerable Marine Ecosystem indicators and protection measures should be adopted as a precautionary approach (Massi et al., 2018).

The population of *C. verticillata* at the SW Flank was composed of two size groups, 65 cm and 86 cm divided respectively into 27% and 73%, both corresponding to tall sizes, with no record of small specimens. Small colonies may be located at another place that we may not have explored. A bi-modal size structure has already been described for *C. verticillata* in the Gulf of S. Eufemia (Tyrrhenian Sea) where colonies of *C. vertcillata* presented two groups of colonies of smaller sizes (15-20 cm or 55-60 cm) (Bo et al., 2012b). At Cassis-500, the size structure of the *C. verticillata* population was divided into three groups of 27, 52 and 87 cm (23%, 32% and 45 %). The presence of small colonies supports the idea of a population with recruitment. Since the medium size class is less abundant than the two others, it may have suffered from the high sedimentation rate of bauxite residues expelled at the site, but now that the discharge of these residues has stopped a new generation may have settled.

The whip gorgonian *V. flagellum* formed large forests at SW Flank and we measured a mean size of 53±19 cm, divided into two groups of 42 and 69 cm (57% and 43%). The measurements may be inaccurate because *V. flagellum* is flexible and the 3D models may not have properly reconstructed the apex of the colonies. No measurement for *V. flagellum* is reported in the literature.

4.4 Diversity of accompanying species

At Cassis-200, a higher megafauna species richness was observed compared to the three other locations in the canyon, and exceptional diversity patterns were associated with the highest topographic elevations (knolls) covered by *M. oculata*, i.e. forests of *A. subpinnata* were found at Knolls 9 and 3; *Paramuricea clavata* was found at Knoll 3; and *C. rubrum* was observed at Knolls 3, 8, 15 and 16. These knolls are high topographic elevations on which species can be exposed to currents. This factor was reported to be a driver of the distribution of deep-water corals, for example *M. oculata* (Fabri et al., 2017; Bargain et al., 2018) and *C. rubrum* (Lastras et al., 2016) in the Mediterranean Sea, but also *Lophelia pertusa* in the Atlantic Ocean (Mohn et al., 2014). The association of the precious red coral *C. rubrum* with the scleractinian *M. oculata* has often been reported in the Mediterranean Sea (Rossi et al., 2008; Costantini et al., 2010; Lastras et al., 2016) and deep occurrences have been discovered recently (Evans et al., 2016; Knittweis et al., 2016). Two scleractinian species, the yellow coral *Dendrophyllia cornigera* and the solitary coral *Dendrophyllium dianthius*, are widely described in association with *M. oculata* in other canyons, such as in the Sardianian canyons (Taviani et al., 2017) and the Levante canyon (Fanelli et al., 2017). The presence of tall colonies of *M. oculata* at Cassis-200, as well as the multi-modal size structure of the population, suggests a healthy population. This exuberant development of colonies is known to provide a habitat structure for many other species (D'Onghia et al., 2012) and may explain the high number of accompanying species of megafauna we recognized (63 species or morphotypes) following Fourt et al. (2017). The presence of *M. oculata* has already been shown to enhance the local diversity of species at a site (D'Onghia et al., 2010). In comparison with lists of species observed at other *M. oculata* locations in the Mediterranean Sea, we observe that fewer than 50 megafauna species are commonly reported in cold-water ecosystems using images only, i.e. 24 megafauna species were reported in the Bari canyon (Angeletti et al., 2014); 30 megafauna species in La Fonera canyon (Lastras et al., 2016). But when using sampling, including megafauna and macrofuana, the number of species increases: e.g. 222 species were identified at Santa Maria di Leuca (Mastrototaro et al., 2010).

At Cassis-500, colonies of *M. oculata* were spaced from each other, growing only on the vertical part of a ledge and not on the top. Accompanying species were less numerous (34 species or morphotypes) than at Cassis-200, and composed of different species (only 48% similarity). Cassis-500 has been impacted by waste disposal for 50 years (Dauvin, 2010; Fabri et al., 2017), and the effects are visible in every video and photo. Therefore, species growing at Cassis-500 are those able to live without being buried and able to cope with sedimentation. Since this site is also the deepest in our study, we cannot exclude the hypothesis that depth could also be a factor explaining a change in species diversity. However, the exceptional diversity found recently deep in the Mediterranean Sea, for example at depths of 400 m in Sardinian canyons (Moccia et al., 2019) or at depths of 1000 m off

Malta (Evans et al., 2016), suggest that depth is not the main factor that prevented accompanying fauna to develop at Cassis-500.

We observed the lowest number of accompanying species at the Wall (23 species or morphotypes) and a similarity of up to 50% with Cassis-200 and SW Flank. We could see *M. oculata* and a blue sponge entirely covering the ceiling of overhangs, and the red coral *C. rubrum* living on the border of the overhang between small colonies of *M. oculata*. A few other species, mainly sponges, have settled on the vertical part of the cliff, but do not specifically accompany *M. oculata*. The difficult navigation conditions encountered along the vertical cliff and the difficulties in observing the ceiling under the overhangs prevented good observation of species, which may explain the low number of species reported in this study. But this location is also the most distant from the coast and from the organic matter input, which may also explain the low number of species.

Forests of *A. subpinata* and gardens of *L. glaberrima* were seen in the vicinity of either *M. oculata* at Cassis-200, or *V. flagellum* at SW Flank. Those two locations presented the highest numbers of megafauna species (respectively 63 and 52 species or morphotypes) and presented a species composition with more than 70% similarity. Antipatharians have already been described as true oases of biodiversity (Bo et al., 2012b). Given their large tree-like structure, antipatharians can form gardens or forests that have been compared to terrestrial forests given their longevity and the amount of high biodiversity they support (Bo et al., 2015). Antipatharians also have a nursery role in the ecosystem (Bo et al., 2015). The fragility of antipatharians has been recognized and the FAO now considers coral gardens as VMEs (FAO, 2016). *Leiopathes glaberrima* appears as an endangered species on the IUCN Red list of species (Bo et al., 2015). The three species of antipatharians observed in the Cassidaigne canyon are protected under three different conventions: CITES (Convention on International Trade in Endangered species), the Bern convention (Treaty no. 104; Bern, 19.IX.1979) and the Barcelona convention (IG.23/10/EC) where antipatharians are listed in Annex II (*L. glaberrima*) and Annex III (*A. subpinnata* and *A. dicthoma*).

Both gorgonian species, *C. vertilliata* and *V. flagellum,* were present as deep forests at SW Flank and may play important habitat structuring roles. We observed gorgonians in association with antipatharians (above paragraph), scleractinians (*D. dianthus* and *D. cornigea*) and commercially important species, such as the seabream *Pagellus bogaraveo* and the lobster *Palinurus mauritanicus*. The presence of epifauna species in the canopy of *C. verticillata* was often seen. A high number of colonies of *C. verticillata* were observed acting as hosts for nudibranchs. A previously identified zoantharian species, *Zibrowius primnoidus*, was reported as a parasite of *C. verticillata* (Carreiro-Silva et al., 2017). This zoantharian is known to use the colony as a host and as a food resource by eating the tissue. Observations of the high abundance of epifauna showing negative effects on colonies of *C. verticillata* have also been demonstrated in Sicilian waters (Bo et al., 2014). In our study, we also observed the presence of the echinoid *C. cidaris* together with necroses in the canopy of *C. vertcillata* at SW Flank, but neither the echinoid nor the gorgonian necroses were seen at Cassis-500. We assume that a relationship exists between the high number of sea urchins and the high number of necroses in the canopies. At Cassis-500 it seems that bauxite residues and sedimentation rate prevent the settlement of *C. cidaris* and therefore its feeding on *C. verticillata*. Bauxite residues could thus protect *C. verticillata* from grazing.

With regards to diversity, caution is necessary when considering the number of megafauna species presented in this study as it was based on photos and video analysis, which can lead to bias and the misidentification of species. Moreover, macrofauna and meiofauna are not considered in our study since no sampling was performed. Quantitative evaluation of diversity was not possible because the species matrix was not quantitative and the only data available was the presence and absence of species. Although the number of species identified at Cassis-200 appears to illustrate high diversity when compared to the three other locations explored in the canyon, the number of species at this location nonetheless remains underestimated. For example, video observations have shown a high abundance and diversity of sponges at Cassis-200, but the species could not be identified, since the identification of sponges requires physical sampling (Bo et al., 2012a), and sometimes genetic analysis (Bakran-Petricioli et al., 2007).

4.5 Seafloor integrity

4.5.1 Marine litter and waste disposal

Marine Litter was mainly composed of plastics at the four locations, reflecting the general trend previously described in French Mediterranean canyons (Fabri et al., 2014; Gerigny et al., 2019). Plastic items were identified as derelict fishing gears such as fishing long lines. They were seen in high abundance in all the coral habitats explored, together with coral rubble. Overall, in Cassidaigne canyon, the surface corresponding to *M. oculata* rubble was measured as 15% of the total surface occupied by the species. It is known that fishing longlines can have impacts on colonies due to entanglement and physical breakage (Lastras et al., 2016; D'Onghia et al., 2017; Fanelli et al., 2017; Galgani et al., 2018). Yet, in Cassidaigne canyon, the locations Cassis-200 and Cassis-500 have been included within regulated fisheries zones since 2012. This indicates that the fishing gears observed during our study, entangled in coral colonies, were lost before that time. Our study took place on the upper part of Cassidaigne canyon's flank, therefore we could not observe heavy litter items as those described in three large submarine canyon off Spain (Tubau et al., 2015), but we found the same distribution of marine debris, mainly composed of longlines, observed between 30 to 300 m in the Tyrrhenian Sea (Angiolillo et al., 2015). These fishing gears were seen colonized by *M. oculata* and similar observations have also been described in the Levante canyon (Fanelli et al., 2017). This shows the persistence of the abandoned fishing gears and the resilience capacities of the ecosystem. The largest surface of coral rubble was found at the Wall, but at this location of coral rubble is more likely caused by the natural fall of the colonies under their own weight than by fishery-related impacts.

Another impact on the *M. oculata* ecosystem in Cassidaigne canyon is the presence of bauxite residues at Cassis-500, covering 56% of the total area where *M. oculata* colonies are known to have settled. It is possible that a non-evaluated part of the habitat was completely buried by bauxite residues, and this would increase the proportion of the ecosystem impacted. At Cassis-500 the local species composition is affected, evidenced by the low number of species observed and the lowest similarity in species composition compared to the three other sites. Moreover, at Cassis-500, the size structure of *M. oculata* population is different from that measured at Cassis-200, and the mean size of colonies is smaller. The gorgonian *C. verticillata* has a size structure with a very low number of colonies in the middle size group, which may correspond to a group of colonies that had settled when industrial wastes were expelled in large quantities. Even though the disposal of waste in solid

particle form was stopped in January 2016 (Fabri et al., 2017), it will take many years before noticeable changes occur.

4.5.2 Seafloor Integrity criteria for the European MSFD

To consider the Good Ecological Status of benthic habitats, the MSFD stipulates the use of descriptor 6, Seafloor Integrity, and more specifically two criteria: the extent of loss of the habitat type (D6C4), and the extent of adverse effects on the condition of the habitat type (D6C5). These criteria measure the degree of anthropogenic effects on biological parameters that should not exceed a specified proportion of the natural extent of the habitat (EU Decision 2017/848). According to the MSFD, the physical loss of the natural seabed due to permanent change of the seabed substrate or morphology should be considered as a permanent change to the seabed that has lasted or is expected to last for a period of two reporting cycles (12 years) or more.

In this study, we considered the habitat type to be the *M. oculata* ecosystem at the scale of the Cassidaigne canyon, and we used photos, videos and photogrammetry to evaluate the status of the ecosystem with the two criteria suggested for benthic habitats. Our results show that the proportion of the habitat impacted by bauxite residues (waste disposal) was 56% of the total extent of the *M. oculata* habitat. This proportion represents the total surface occupied by *M. oculata* at Cassis-500, where we can attest that in the deepest part, *M. oculata* colonies were completely dead; the density of the structuring species *M. oculata* is lower compared to the other sites in the canyon; the mean sizes of the structuring species *M. oculata* and *C. verticillata* are smaller than the size at visually non-impacted sites; the size structure of these populations (*M. oculata* and *C. verticillata*) is different compared to the size structure at visually non-impacted sites; the accompanying species presented a particular and different composition, compared to visually non-impacted sites in the canyon.

It is noteworthy that a 12-year interval in the deep sea is very short and the impact on the deep seafloor is of much greater concern than on the continental shelf because of the low resilience of deep-sea benthic ecosystems (Fabri et al., 2018). We can therefore conclude that in the light of criterion D6C4, the extent of loss of the *M. oculata* ecosystem equals 56% in the Cassidaigne canyon and will need more than 12 years to recover despite the fact that the pressure has stopped.

4.6 Temporal changes

The MSFD advises that special conservation areas should be monitored every 6 years to evaluate the Ecological Status of European marine waters (EC 734/2008). In our study, we presented an attempt to perform a temporal analysis at 7 and 5 year intervals on two luxuriant *M. oculata* knolls at Cassis-200. Using 3D models of 2017 made it possible to recognise which knolls had been observed in 2010 and 2013 and to compare them with what we observed in 2017. It was difficult to quantify changes in the general size and distribution of *M. oculata* colonies, and sizes could not be quantified because we did not possess good resolution images for the 2010 and 2013 cruises, and because videos were not recorded with the objective to build 3D models, we could not quantify sizes. In addition, the low growth rate and low fecundity of *M. oculata*, explain the small changes seen between years. Therefore, based on these results we suggest that if legal conservation instruments are applied in the area, instead of the 6-year monitoring cycles considered by the MSFD, a 12-year monitoring cycle

should be enough for *M. oculata* ecosystems at Cassis-200. Monitoring should be strengthened at Cassis-500, where recovery should be observed in terms of species diversity since the disposal of bauxite residues was stopped in 2016. However, although the necessary time for the recovery is not known, this site could be a good observatory. Obviously, in the deepest part of the site, where hard bottoms are covered by bauxite residues, sessile benthic species will probably never be able to settle again.

4.7 Validation of potential habitat maps

The suitable habitats predicted previously in Cassidaigne canyon with statistical models (Fabri et al., 2017; Bargain et al., 2018) were visually explored during the Videocor1 2017 cruise described in our study. At every location predicted to be a probable habitat for *M. oculata* we found large cnidarian species able to play a structural role in the ecosystems, i.e. *M. oculata* or antipatharians or large gorgonians. At SW Flank we did not find the exact species we expected to find, therefore we can hypothesize that: (1) the parameters used as drivers for the distribution of *M. oculata* are the same for the different species of cnidarians and we may not have elucidated the parameters strictly related to the scleractinians; (2) and if the parameters are the same, competition between species may have led to one species dominating instead of another. For example, at SW Flank where we expected to find *M. oculata* populations but where we saw large forests of antipatharians and gorgonians, it may be that every hard substrate available for the establishment of *M. oculata* was already occupied by antipatharians and gorgonians, therefore we saw only sparse colonies of *M. oculata*. Whatever the case we found habitat-forming species of cnidarians sheltering a diverse ecosystem where potential areas for cold-water corals were predicted.

5. Conclusion

Photogrammetry provided much information on the complex locations in Cassidaigne canyon. Every site/location can now be easily recognized by its particular shape, and 3D models helped to better understand where vulnerable ecosystems are located. Moreover, the detailed maps produced in this work will be of great help for future monitoring of the area. Also, the precise navigation now possible with ROVs and submersibles allows exact positioning and returning to study locations very easily, ensuring repeatability in the methodology. In a world in which the number of impacts on marine environments is increasing, and in which assessments sometimes use methodologies like sampling that damage marine ecosystems, innovative non-intrusive methods such as imagery and 3D models can be used to better understand protected habitats. Photogrammetry is therefore a good means of obtaining quantitative data in the deep sea and of better calculating surfaces, densities and size parameters. However, it is noteworthy that density results correspond to an estimation limited by several methodological factors. First, the number of colonies counted and the measurement of surface areas were limited to the areas reconstructed in 3-dimensions. Second, the number of colonies plotted in 3D corresponded to an approximation of their total number, and this number is underestimated, especially in 3D models built from video data where the low image resolution makes it difficult to identify every colony. Third, in sites with dense agglomerations of colonies it was difficult to distinguish and count individual ones. Additionally, there is a substantial risk of not

plotting colonies of small size due to misidentification. Nonetheless, this methodology allows comparing quantitative data between sites and monitoring their evolution through time. 3D models built at regular intervals will allow monitoring vulnerable ecosystems, giving access to distribution, density and size parameters.

ACKNOWLEDGEMENTS

This paper was written in the framework of the IDEM European project (Implementation of the second cycle of the marine strategy framework directive www.msfd-idem.eu) No. 11.0661/2017/750680/SUB/ENV.C2. Part of this work was performed by B. V. in the framework of an International MSc in Marine Biodiversity and Conservation. We are grateful to all the participants of VIDEOCOR1 cruise in 2017 (https://doi.org/10.17600/17004700 and https://doi.org/10.17600/17005400) and the BATHYCOR2 cruise in 2016 (https://doi.org/10.17600/16011300). Furthermore, we are indebted to Keith Hodson (http://www.accent-europe.fr) for correcting the English. The authors also thank the reviewers for their helpful comments aimed at improving the manuscript.

REFERENCES

Addinsoft, 2019. XLSTAT statistical and data analysis solution, Long Island, NY, USA. https://www.xlstat.com.,

Alberola, C., Millot, C., 2003. Circulation in the French Mediterranean coastal zone near Marseilles: the influence of wind and the Northern Current, Continental Shelf Research 23, 6, 587-610, https://doi.org/10.1016/s0278-4343(03)00002-5

Angeletti, L., Mecho, A., Doya, C., Micallef, A., Huvenne, V., Georgiopoulou, A., Taviani, M., 2015. First report of live deep-water cnidarian assemblages from the Malta Escarpment, Italian Journal of Zoology 82, 2, 291-297, https://doi.org/10.1080/11250003.2015.1026416

Angeletti, L., Taviani, M., Canese, S., Foglini, F., Mastrototaro, F., Argnani, A., Trincardi, F., Bakran-Petricioli, T., Ceregato, A., Chimienti, G., et al., 2014. New deep-water cnidarian sites in the southern Adriatic Sea, Mediterranean Marine Science 15, 2, 263-273, https://doi.org/10.12681/mms.558

Angiolillo, M., Bavestrello, G., Bo, M., Cau, A., Giusti, M., Salvati, E., Tunesi, L., Canese, S., 2014. Distribution of the deep-dwelling gorgonian Viminella flagellum in the Italian western Mediterranean sea by means of multi-year ROV surveys, 1st Mediterranean symposium on the conservation of Dark Habitats, Portorož, Slovenia.

Angiolillo, M., Lorenzo, B.d., Farcomeni, A., Bo, M., Bavestrello, G., Santangelo, G., Cau, A., Mastascusa, V., Cau, A., Sacco, F., et al., 2015. Distribution and assessment of marine debris in the deep Tyrrhenian Sea (NW Mediterranean Sea, Italy), Marine Pollution Bulletin 92, 1–2, 149-159, https://doi.org/10.1016/j.marpolbul.2014.12.044

Arnaubec, A., Opderbecke, J., Allais, A.G., Brignone, L., 2015. Optical mapping with the ARIANE HROV at IFREMER: The MATISSE processing tool, OCEANS 2015 - Genova, 1-6, https://doi.org/10.1109/OCEANS-Genova.2015.7271713

Bakran-Petricioli, T., Vacelet, J., Zibrowius, H., Petricioli, D., Chevaldonne, P., Rada, T., 2007. New data on the distribution of the 'deep-sea' sponges *Asbestopluma hypogea* and *Oopsacas minuta* in the Mediterranean Sea, Marine Ecology-an Evolutionary Perspective 28, 10-23, https://doi.org/10.1111/j.1439-0485.2007.00179.x

Bargain, A., Foglini, F., Pairaud, I., Bonaldo, D., Carniel, S., Angeletti, L., Taviani, M., Rochette, S., Fabri, M.C., 2018. Predictive habitat modeling in two Mediterranean canyons including hydrodynamic variables, Progress in Oceanography, https://doi.org/10.1016/j.pocean.2018.02.015

Benn, A.R., Weaver, P.P., Billet, D.S.M., van den Hove, S., Murdock, A.P., Doneghan, G.B., Le Bas, T., 2010. Human Activities on the Deep Seafloor in the North East Atlantic: An Assessment of Spatial Extent, Plos One 5, 9, https://doi.org/10.1371/journal.pone.0012730

Bo, M., Barucca, M., Biscotti, M.A., Brugler, M.R., Canapa, A., Canese, S., Lo Iacono, C., Bavestrello, G., 2018. Phylogenetic relationships of Mediterranean black corals (Cnidaria:Anthozoa:Hexacorallia) and implications for classification within the order Antipatharia, Invertebrate Systematics 32, 5, 1102-1110, https://doi.org/10.1071/is17043

Bo, M., Bavestrello, G., Angiolillo, M., Calcagnile, L., Canese, S., Cannas, R., Cau, A., D'Elia, M., D'Oriano, F., Follesa, M.C., et al., 2015. Persistence of Pristine Deep-Sea Coral Gardens in the Mediterranean Sea (SW Sardinia), Plos One 10, 3, e0119393, https://doi.org/10.1371/journal.pone.0119393

Bo, M., Bavestrello, G., Canese, S., Giusti, M., Angiolillo, M., Cerrano, C., Salvati, E., Greco, S., 2011. Coral assemblage off the Calabrian Coast (South Italy) with new observations on living colonies of Antipathes dichotoma, Italian Journal of Zoology 78, 2, 231-242, https://doi.org/10.1080/11250001003652619

Bo, M., Bavestrello, G., Canese, S., Giusti, M., Salvati, E., Angiolillo, M., Greco, S., 2009. Characteristics of a black coral meadow in the twilight zone of the central Mediterranean Sea, Marine Ecology-Progress Series 397, 53-61, https://doi.org/10.3354/meps08185

Bo, M., Bertolino, M., Bavestrello, G., Canese, S., Giusti, M., Angiolillo, M., Pansini, M., Taviani, M., 2012a. Role of deep sponge grounds in the Mediterranean Sea: a case study in southern Italy, Hydrobiologia 687, 1, 163-177, https://doi.org/10.1007/s10750-011-0964-1

Bo, M., Canese, S., Spaggiari, C., Pusceddu, A., Bertolino, M., Angiolillo, M., Giusti, M., Loreto, M.F., Salvati, E., Greco, S., et al., 2012b. Deep coral oases in the South Tyrrhenian Sea, Plos One 7, 11, e49870, https://doi.org/10.1371/journal.pone.0049870

Bo, M., Cerrano, C., Canese, S., Salvati, E., Angiolillo, M., Santangelo, G., Bavestrello, G., 2014. The coral assemblages of an off-shore deep Mediterranean rocky bank (NW Sicily, Italy), Marine Ecology-an Evolutionary Perspective 35, 3, 332-342, https://doi.org/10.1111/maec.12089

Boury-Esnault, N., Vacelet, J., Dubois, M., Goujard, A., Fourt, M., Perez, T., Chevaldonne, P., 2017. New hexactinellid sponges from deep Mediterranean canyons, Zootaxa 4236, 1, 118-134, https://doi.org/10.11646/zootaxa.4236.1.6

Bruno, F., Bianco, G., Muzzupappa, M., Barone, S., Razionale, A.V., 2011. Experimentation of structured light and stereo vision for underwater 3D reconstruction, Isprs Journal of Photogrammetry and Remote Sensing 66, 4, 508-518, https://doi.org/10.1016/j.isprsjprs.2011.02.009

Carlier, A., Le Guilloux, E., Olu, K., Sarrazin, J., Mastrototaro, F., Taviani, M., Clavier, J., 2009. Trophic relationships in a deep Mediterranean cold-water coral bank (Santa Maria di Leuca, Ionian Sea), Mar. Ecol. Prog. Ser. 397, 125-137, https://doi.org/10.3354/meps08361

Carreiro-Silva, M., Andrews, A.H., Braga-Henriques, A., de Matos, V., Porteiro, F.M., Santos, R.S., 2013. Variability in growth rates of long-lived black coral Leiopathes sp. from the Azores, Mar. Ecol. Prog. Ser. 473, 189-199, https://doi.org/10.3354/meps10052

Carreiro-Silva, M., Ocaña, O., Stanković, D., Sampaio, Í., Porteiro, F.M., Fabri, M.-C., Stefanni, S., 2017. Zoantharians (Hexacorallia: Zoantharia) Associated with Cold-Water Corals in the Azores Region: New Species and Associations in the Deep Sea, Frontiers in Marine Science 4, 88, https://doi.org/10.3389/fmars.2017.00088

Cau, A., Bramanti, L., Cannas, R., Follesa, M., Angiolillo, M., Canese, S., Bo, M., Cuccu, D., Guizien, K., 2016. Habitat constraints and self-thinning shape Mediterranean red coral deep population structure: Implications for conservation practice. https://www.nature.com/articles/srep23322

Cau, A., Moccia, D., Follesa, M.C., Alvito, A., Canese, S., Angiolillo, M., Cuccu, D., Bo, M., Cannas, R., 2017. Coral forests diversity in the outer shelf of the south Sardinian continental margin, Deep-Sea Research Part I-Oceanographic Research Papers 122, 60-70, https://doi.org/10.1016/j.dsr.2017.01.016

Claudet, J., Fraschetti, S., 2010. Human-driven impacts on marine habitats: A regional meta-analysis in the Mediterranean Sea, Biological Conservation 143, 9, 2195-2206, https://doi.org/10.1016/j.biocon.2010.06.004

Costantini, F., Taviani, M., Remia, A., Pintus, E., Schembri, P.J., Abbiati, M., 2010. Deep-water *Corallium rubrum* (L., 1758) from the Mediterranean Sea: preliminary genetic characterisation, Marine Ecology 31, 2, 261-269, https://doi.org/10.1111/j.1439-0485.2009.00333.x

Costello, M.J., McCrea, M., Freiwald, A., Lundalv, T., Jonsson, L., Bett, B.J., van Weering, T.C.E., de Haas, H., Roberts, J.M., Allen, D., 2005. Role of cold-water Lophelia pertusa coral reefs as fish habitat in the NE

Atlantic.[Freiwald, A.R.J.M. (Ed.)] Cold-Water Corals and Ecosystems, pp. 771-805, https://doi.org/10.1007/3-540-27673-4_41. 3-540-24136-1

D'Onghia, G., Calculli, C., Capezzuto, F., Carlucci, R., Carluccio, A., Grehan, A., Indennidate, A., Maiorano, P., Mastrototaro, F., Pollice, A., et al., 2017. Anthropogenic impact in the Santa Maria di Leuca cold-water coral province (Mediterranean Sea): Observations and conservation straits, Deep-Sea Research Part Ii-Topical Studies in Oceanography 145, 87-101, https://doi.org/10.1016/j.dsr2.2016.02.012

D'Onghia, G., Maiorano, P., Carlucci, R., Capezzuto, F., Carluccio, A., Tursi, A., Sion, L., 2012. Comparing Deep-Sea Fish Fauna between Coral and Non-Coral "Megahabitats" in the Santa Maria di Leuca Cold-Water Coral Province (Mediterranean Sea), Plos One 7, 9, e445090, https://doi.org/10.1371/journal.pone.0044509

D'Onghia, G., Maiorano, P., Sion, L., Giove, A., Capezzuto, F., Carlucci, R., Tursi, A., 2010. Effects of deep-water coral banks on the abundance and size structure of the megafauna in the Mediterranean Sea, Deep-Sea Research II 57, 5-6, 397-411, https://doi.org/10.1016/j.dsr2.2009.08.022

Dauvin, J.C., 2010. Towards an impact assessment of bauxite red mud waste on the knowledge of the structure and functions of bathyal ecosystems: The example of the Cassidaigne canyon (north-western Mediterranean Sea), Marine Pollution Bulletin 60, 2, 197-206, https://doi.org/10.1016/j.marpolbul.2009.09.026

Deidun, A., Andaloro, F., Bavestrello, G., Canese, S., Consoli, P., Micallef, A., Romeo, T., Bo, M., 2015. First characterisation of a Leiopathes glaberrima (Cnidaria: Anthozoa: Antipatharia) forest in Maltese exploited fishing grounds, Italian Journal of Zoology 82, 2, 271-280, https://doi.org/10.1080/11250003.2014.986544

European Commission, 2017a. Decision (EU) 2017/848 laying down criteria and methodological standards on good environmental status of marine waters ans specifications and standardised methods for monitoring and assessment, and repealing Decision 2010/477/EU. Official journal of the European Union, 43-74, http://data.europa.eu/eli/dec/2017/848/oj

European Commission, 2017b. Directive (EU) 2017/845 amending Directive 2008/56/EC of the European Parliament and of the Council as regards the indicative lists of elements to be taken into account for the preparation of marine strategies. Official journal of the European Union, 27-33, http://data.europa.eu/eli/dir/2017/845/oj

European Commission, S., 2013. Executive Summary of the Impact Assessment accompanying the document 'Proposal for a regulation of the European Parliament and of the Council on the prevention and management of the introduction and spread of invasive alien species'. 322, http://eur-lex.europa.eu/legal-content/EN/ALL/?uri=CELEX:52013SC0322

European Parliament, 2008. Directive (2008/56/EC) establishing a framework for community action in the field of marine environmental policy (Marine Strategy Framework Directive). Official journal of the European Union, 1-22, http://data.europa.eu/eli/dir/2008/56/oj

Evans, J., Aguilar, R., Alvarez, H., Borg, J.A., Garcia, S., Knittweis, L., Schembri, P.J., 2016. Recent evidence that the deep sea around Malta is a biodiversity hotspot. Rapport du Congrès de la Commission Internationale pour l'Exploitation Scientifique de la Mer Méditerranée 41, 463

Fabri, M.-C., Brind'Amour, A., Jadaud, A., Galgani, F., Vaz, S., Taviani, M., Scarcella, G., Canals, M., Sanchez, A., Grimalt, J., et al., 2018. Review of literature on the implementation of the MSFD to the deep Mediterranean Sea. Ifremer, 10.13155/53809, https://archimer.ifremer.fr/doc/00426/53809/

Fabri, M.C., Bargain, A., Pairaud, I., Pedel, L., Taupier-Letage, I., 2017. Cold-water coral ecosystems in Cassidaigne Canyon: An assessment of their environmental living conditions, Deep Sea Research Part II: Topical Studies in Oceanography 137, 436-453, https://doi.org/10.1016/j.dsr2.2016.06.006

Fabri, M.C., Pedel, L., Beuck, L., Galgani, F., Hebbeln, D., Freiwald, A., 2014. Megafauna of vulnerable marine ecosystems in French mediterranean submarine canyons: Spatial distribution and anthropogenic impacts, Deep-Sea Research Part Ii-Topical Studies in Oceanography 104, 184-207, https://doi.org/10.1016/j.dsr2.2013.06.016

Fanelli, E., Delbono, I., Ivaldi, R., Pratellesi, M., Cocito, S., Peirano, A., 2017. Cold-water coral Madrepora oculata in the eastern Ligurian Sea (NW Mediterranean): Historical and recent findings, Aquat. Conserv.: Mar. Freshwat. Ecosyst., 1-11, https://doi.org/10.1002/aqc.2751

FAO, 2016. Vulnerable Marine Ecosystems : Processes and Practices in the High Seas. FAO Fisheries and Aquaculture Technical Paper No. 595, www.fao.org/3/a-i5952e.pdf

Fontanier, C., Biscara, L., Mamo, B., Delord, E., 2015. Deep-sea benthic foraminifera in an area around the Cassidaigne Canyon (NW Mediterranean) affected by bauxite discharges, Marine Biodiversity 44, 4, https://doi.org/10.1007/s12526-014-0281-9

Fontanier, C., Fabri, M.C., Buscail, R., Biscara, L., Koho, K., Reichart, G.J., Cossa, D., Galaup, S., Chabaud, G., Pigot, L., 2012. Deep-sea foraminifera from the Cassidaigne Canyon (NW Mediterranean): Assessing the environmental impact of bauxite red mud disposal, Marine Pollution Bulletin 64, 9, 1895-1910, https://doi.org/10.1016/j.marpolbul.2012.06.016

Fourt, M., Goujard, A., Pérez, T., Chevaldonnée, P., 2017. Guide de la faune profonde de la mer Méditerranée. Explorations des roches et canyons sous-marins des côtes françaises., (Patrimoines Naturels; 75) ed. Museum national d'Histoire naturelle, Paris, 184 p., 978-2-85653-802-9. http://sciencepress.mnhn.fr/fr/collections/patrimoines-naturels/guide-de-la-faune-profonde-de-la-mer-mediterranee

Freiwald, A., Beuck, L., Rüggeberg, A., Taviani, M., Hebbeln, D., 2009. The white coral community in the Central Mediterranean Sea revealed by ROV Surveys, Oceanography 22, 1, 58-74, https://doi.org/dx.doi.org/10.5670/oceanog.2009.06

Freiwald, A., Fossa, J.H., Grehan, A., Koslow, J.A., Roberts, J.M., 2004. Cold-water Coral Reefs: Out of Sight - No Longer Out of Mind. UNEP-WCMC, Cambridge, UK. http://www.unep-wcmc.org/biodiversity-series-22_103.html

Galgani, F., Pham, C.K., Claro, F., Consoli, P., 2018. Marine animal forests as useful indicators of entanglement by marine litter, Marine Pollution Bulletin 135, 735-738, https://doi.org/10.1016/j.marpolbul.2018.08.004

Galli, G., Bramanti, L., Priori, C., Rossi, S., Santangelo, G., Tsounis, G., Solidoro, C., 2016. Modelling red coral (Corallium rubrum) growth in response to temperature and nutrition, Ecological Modelling 337, 137-148, https://doi.org/10.1016/j.ecolmodel.2016.06.010

Gerigny, O., Brun, M., Fabri, M.C., Tomasino, C., Le Moigne, M., Jadaud, A., Galgani, F., 2019. Seafloor litter from the continental shelf and canyons in French Mediterranean Water: Distribution, typologies and trends, Marine Pollution Bulletin 146, 653-666, https://doi.org/10.1016/j.marpolbul.2019.07.030

Giusti, M., Bo, M., Angiolillo, M., Cannas, R., Cau, A., Follesa, M.C., Canese, S., 2017. Habitat preference of Viminella flagellum (Alcyonacea: Ellisellidae) in relation to bathymetric variables in southeastern Sardinian waters, Continental Shelf Research 138, 41-50, https://doi.org/10.1016/j.csr.2017.03.004

Giusti, M., Bo, M., Bavestrello, G., Angiolillo, M., Salvati, E., Canese, S., 2012. Record of Viminella flagellum (Alcyonacea: Ellisellidae) in Italian waters (Mediterranean Sea), Marine Biodiversity Records 5, https://doi.org/10.1017/S1755267211000510

Gori, A., Orejas, C., Madurell, T., Bramanti, L., Martins, M., Quintanilla, E., Marti-Puig, P., Lo Iacono, C., Puig, P., Requena, S., et al., 2013. Bathymetrical distribution and size structure of cold-water coral populations in the Cap de Creus and Lacaze-Duthiers canyons (northwestern Mediterranean), Biogeosciences 10, 3, 2049-2060, https://doi.org/10.5194/bg-10-2049-2013

Guinotte, J.M., Orr, J., Cairns, S., Freiwald, A., Morgan, L., George, R., 2006. Will human-induced changes in seawater chemistry alter the distribution of deep-sea scleractinian corals?, Frontiers in Ecology and the Environment 4, 3, 141-146, https://doi.org/10.1890/1540-9295(2006)004[0141:whcisc]2.0.co;2

Henry, L.A., Roberts, J.M., 2017. Global Biodiversity in Cold-Water Coral Reef Ecosystems.[Rossi, S., Bramanti, L., Gori, A., Orejas, C. (Eds.)] Marine Animal Forests, p. 1369, Springer International Publishing. ISBN: 978-3-319-17001-5

Ingrassia, M., Macelloni, L., Bosman, A., Chiocci, F.L., Cerrano, C., Martorelli, E., 2016. Black coral (Anthozoa, Antipatharia) forest near the western Pontine Islands (Tyrrhenian Sea), Marine Biodiversity 46, 1, 285-290, https://doi.org/10.1007/s12526-015-0315-y

Knittweis, L., Aguilar, R., Alvarez, H., Borg, J.A., Evans, J., Garcia, S., Schembri, P.J., 2016. New depth record of the precious red coral *Corallium rubrum* for the Mediterranean. Rapport du Congrès de la Commission Internationale pour l'Exploitation Scientifique de la Mer Méditerranée 41

Lastras, G., Canals, M., Ballesteros, E., Gili, J.M., Sanchez-Vidal, A., 2016. Cold-Water Corals and Anthropogenic Impacts in La Fonera Submarine Canyon Head, Northwestern Mediterranean Sea, Plos One 11, 5, https://doi.org/10.1371/journal.pone.0155729

Massi, D., Vitale, S., Titone, A., Milisenda, G., Gristina, M., Fiorentino, F., 2018. Spatial distribution of the black coral Leiopathes glaberrima (Esper, 1788) (Antipatharia: Leiopathidae) in the Mediterranean: a prerequisite for protection of Vulnerable Marine Ecosystems (VMEs), The European Zoological Journal 85, 1, 170-179, https://doi.org/10.1080/24750263.2018.1452990

Mastrototaro, F., D'Onghia, G., Corriero, G., Matarrese, A., Maiorano, P., Panetta, P., Gherardi, M., Longo, C., Rosso, A., Sciuto, F., et al., 2010. Biodiversity of the white coral bank off Cape Santa Maria di Leuca (Mediterranean Sea): An update, Deep Sea Research Part II 57, 5-6, 412-430, https://doi.org/10.1016/j.dsr2.2009.08.021

McCulloch, M., Trotter, J., Montagna, P., Falter, J., Dunbar, R., Freiwald, A., Försterra, G., López Correa, M., Maier, C., Rüggeberg, A., et al., 2012. Resilience of cold-water scleractinian corals to ocean acidification: Boron isotopic systematics of pH and saturation state up-regulation, Geochimica Et Cosmochimica Acta 87, 21-34, https://doi.org/10.1016/j.gca.2012.03.027

Millot, C., 1990. The Gulf of Lions' hydrodynamics, Continental Shelf Research 10, 9-11, 885-894, https://doi.org/10.1016/0278-4343(90)90065-T

Moccia, D., Cau, A., Alvito, A., Canese, S., Cannas, R., Bo, M., Angiolillo, M., Follesa, M.C., 2019. New sites expanding the "Sardinian cold-water coral province" extension: A new potential cold-water coral network?, Aquat. Conserv.: Mar. Freshwat. Ecosyst. 29, 1, 153-160, https://doi.org/10.1002/aqc.2975

Mohn, C., Rengstorf, A., White, M., Duineveld, G., Mienis, F., Soetaert, K., Grehan, A., 2014. Linking benthic hydrodynamics and cold-water coral occurrences: A high-resolution model study at three cold-water coral provinces in the NE Atlantic, Progress in Oceanography 122, 92-104, https://doi.org/10.1016/j.pocean.2013.12.003

Mytilineou, C., Smith, C.J., Anastasopoulou, A., Papadopoulou, K.N., Christidis, G., Bekas, P., Kavadas, S., Dokos, J., 2014. New cold-water coral occurrences in the Eastern Ionian Sea: Results from experimental long line fishing, Deep-Sea Research Part Ii-Topical Studies in Oceanography 99, 146-157, https://doi.org/10.1016/j.dsr2.2013.07.007

OCEANA, 2011. OSPAR workshop on the improvement of the definitions of habitats on the OSPAR list. Bergen, Norway. http://eu.oceana.org/en/publications/reports/ospar-workshop-improvement-definitions-habitats-ospar-list

Orejas, C., Gori, A., Gili, J.M., 2008. Growth rates of live *Lophelia pertusa* and *Madrepora oculata* from the Mediterranean Sea maintained in aquaria, Coral Reefs 27, 2, 255-255, https://doi.org/10.1007/s00338-007-0350-7

Orejas, C., Gori, A., Lo Iacono, C., Puig, P., Gili, J.M., Dale, M.R.T., 2009. Cold-water corals in the Cap de Creus canyon, northwestern Mediterranean: spatial distribution, density and anthropogenic impact, Marine Ecology-Progress Series 397, 37-51, https://doi.org/10.3354/mep08314

Palma, M., Casado, M.R., Pantaleo, U., Pavoni, G., Pica, D., Cerrano, C., 2018. SfM-Based Method to Assess Gorgonian Forests (Paramuricea clavata (Cnidaria, Octocorallia)), Remote Sensing 10, 7, https://doi.org/10.3390/rs10071154

Pires, D.O., Silva, J.C., Bastos, N.D., 2014. Reproduction of deep-sea reef-building corals from the southwestern Atlantic, Deep Sea Research Part II: Topical Studies in Oceanography 99, 51-63, https://doi.org/10.1016/j.dsr2.2013.07.008

Puig, P., Canals, M., Company, J.B., Martin, J., Amblas, D., Lastras, G., Palanques, A., Calafat, A.M., 2012. Ploughing the deep sea floor, Nature 489, 7415, 286-289, https://doi.org/10.1038/nature11410

Raugel, E., Opderbecke, J., Fabri, M.C., Brignone, L., Rigaud, V., 2019. Operational and scientific capabilities of Ariane, Ifremer's hybrid ROV, OCEANS 2019, 1-7, https://proceedings.oceans19mtsieeemarseille.org/session.cfm?sid=76.

Reveillaud, J., Allewaert, C., Pérez, T., Vacelet, J., Banaigs, B., Vanreusel, A., 2012. Relevance of an integrative approach for taxonomic revision in sponge taxa: case study of the shallow-water Atlanto-Mediterranean Hexadella species (Porifera : Ianthellidae : Verongida), Invertebrate Systematics 26, 3, 230-248, https://doi.org/dx.doi.org/10.1071/IS11044

Roark, E.B., Guilderson, T.P., Dunbar, R.B., Fallon, S.J., Mucciarone, D.A., 2009. Extreme longevity in proteinaceous deep-sea corals, Proceedings of the National Academy of Sciences of the United States of America 106, 13, 5204-5208, https://doi.org/10.1073/pnas.0810875106

Robert, K., Huvenne, V.A.I., Georgiopoulou, A., Jones, D.O.B., Marsh, L., Carter, G.D.O., Chaumillon, L., 2017. New approaches to high-resolution mapping of marine vertical structures, Scientific Reports 7, https://doi.org/10.1038/s41598-017-09382-z

Roberts, J.M., Cairns, S.D., 2014. Cold-water corals in a changing ocean, Current Opinion in Environmental Sustainability 7, 118-126, https://doi.org/10.1016/j.cosust.2014.01.004

Roberts, J.M., Long, D., Wilson, J.B., Mortensen, P.B., Gage, J.D., 2003. The cold-water coral Lophelia pertusa (Scleractinia) and enigmatic seabed mounds along the north-east Atlantic margin: are they related?, Marine Pollution Bulletin 46, 1, 7-20, https://doi.org/10.1016/s0025-326x(02)00259-x

Rossi, S., Tsounis, G., Orejas, C., Padron, T., Gili, J.M., Bramanti, L., Teixido, N., Gutt, J., 2008. Survey of deep-dwelling red coral (*Corallium rubrum*) populations at Cap de Creus (NW Mediterranean), Marine Biology 154, 3, 533-545, https://doi.org/10.1007/s00227-008-0947-6

Royer, J.P., Nawaf, M.M., Merad, D., Saccone, M., Bianchimani, O., Garrabou, J., Ledoux, J.B., Lopez-Sanz, A., Drap, P., 2018. Photogrammetric Surveys and Geometric Processes to Analyse and Monitor Red Coral Colonies, Journal of Marine Science and Engineering 6, 2, https://doi.org/10.3390/jmse6020042

Taviani, M., Angeletti, L., Canese, S., Cannas, R., Cardone, F., Cau, A., Cau, A.B., Follesa, M.C., Marchese, F., Montagna, P., et al., 2017. The "Sardinian cold-water coral province" in the context of the Mediterranean coral ecosystems, Deep Sea Research Part II: Topical Studies in Oceanography 145, Supplement C, 61-78, https://doi.org/10.1016/j.dsr2.2015.12.008

Tsounis, G., Rossi, S., Aranguren, M., Gili, J.M., Arntz, W., 2006. Effects of spatial variability and colony size on the reproductive output and gonadal development cycle of the Mediterranean red coral (*Corallium rubrum* L.), Marine Biology 148, 3, 513-527, https://doi.org/10.1007/s00227-005-0100-8

Tubau, X., Canals, M., Lastras, G., Rayo, X., Rivera, J., Amblas, D., 2015. Marine litter on the floor of deep submarine canyons of the Northwestern Mediterranean Sea: The role of hydrodynamic processes, Progress in Oceanography 134, 379-403, https://doi.org/10.1016/j.pocean.2015.03.013

van den Beld, I.M.J., Bourillet, J.-F., Arnaud-Haond, S., de Chambure, L., Davies, J.S., Guillaumont, B., Olu, K., Menot, L., 2017. Cold-Water Coral Habitats in Submarine Canyons of the Bay of Biscay, Frontiers in Marine Science 4, 118, https://doi.org/10.3389/fmars.2017.00118

Wienberg, C., Hebbeln, D., Fink, H.G., Mienis, F., Dorschel, B., Vertino, A., Lopez Correa, M., Freiwald, A., 2009. Scleractinian cold-water corals in the Gulf of Cadiz-First clues about their spatial and temporal distribution, Deep-Sea Research Part I-Oceanographic Research Papers 56, 10, 1873-1893, https://doi.org/10.1016/j.dsr.2009.05.016